2023

Biotic And Abiotic Factors Associated With Temporal And Spatial Variability Of Constitutive Mixotroph Abundance And Proportion

Marcella Dobbertin da Costa
College of William and Mary - Virginia Institute of Marine Science, marcelladcosta1997@gmail.com

Biotic and Abiotic Factors Associated with Temporal and Spatial Variability of Constitutive Mixotroph Abundance and Proportion

---

A Thesis

Presented to

The Faculty of the School of Marine Science

William & Mary

In Partial Fulfillment

of the Requirements for the Degree of

Master of Science

---

by

Marcella Dobbertin da Costa

May 2023

APPROVAL PAGE

This Thesis is submitted in partial fulfillment of

the requirements for the degree of

Master of Science

Marcella Dobbertin da Costa

Approved by the Committee, May 2023

Nicole C. Millette, Ph.D.
Committee Chair / Advisor

Kimberly S. Reece, Ph.D.

Mark J. Brush, Ph.D.

Bongkeun Song, Ph.D.

Rebecca J. Gast, Ph.D.
Woods Hole Oceanographic Institution
Woods Hole, MA, U.S.A.

TABLE OF CONTENTS

ACNK NOWLEDGEMENTS

I would like to acknowledge my adviser Dr. Nicole Millette who has been pivotal in my educational and professional career. I would also like to give special acknowledgement to Dr. Rebecca Gast who has tremendously helped me throughout my career. Dr. Gast provided me with the training and tools to be able to succeed in the molecular component of this project.

I would like to thank Heather Corson for all her help during sampling season. Heather accompanied me numerous times during field sampling. I would also like to thank Michael Lane for all formatted Chesapeake Bay Program historical data he provided.

Lastly, I would like to thank my husband Samuel Marquez for all his help during sampling season. I would also like to thank my friends and family for all their support throughout completing my degree.

LIST OF TABLES

LIST OF FIGURES

Figure A3. Proportion of estimated potential CMs composed of 4 major taxa groups identified through microscopy at (a) RET4.2 and (b) WE4.2.

ABSTRACT

Mixotrophic protists, which combine the use of photosynthesis and prey ingestion to obtain nutrients for growth, comprise a substantial portion of the plankton community. However, there is a major gap in our understanding of how mixotroph prevalence varies spatially and temporally and under what conditions they dominate. I utilized a recently developed molecular technique to experimentally identify active mixotrophs (taxa identified to be grazing when samples were collected) and combined this with microscopy data to estimate active mixotroph abundance and proportion at two locations in a temperate estuary over a year. Active mixotroph abundance was compared to potential mixotroph (taxa that have demonstrated mixotrophic capability in previous peer-reviewed studies) abundance to assess potential overestimations of mixotrophs when not accounting for which taxa are actively ingesting. Measurements of potential mixotrophs demonstrated overestimations of mixotroph abundance. More importantly, analyses demonstrated that presence of taxa with mixotrophic capability does not necessarily mean they are engaging in mixotrophic activity. Constraining the identification of mixotrophs to known active mixotrophs present in the same environment combined with environmental conditions conducive to mixotrophy provides the most accurate estimation of the abundance and proportion of mixotrophs. The abundance of active mixotrophs at both locations was correlated to the abundance of major taxonomic groups. At one location, dinoflagellates were the dominant mixotrophic ASVs throughout the whole year, and the environmental patterns associated with a high abundance of active mixotrophs were similar with the patterns associated with a high abundance of dinoflagellates. At the other location, dinoflagellates and cryptophytes were the dominant mixotrophic ASVs depending upon the time of year, and the environmental patterns associated with a high abundance of mixotrophs were similar to patterns associated with a high abundance of cryptophytes. The results obtained suggest that *in situ* mixotroph abundance might not be only regulated by environmental conditions favorable to mixotrophy but, instead, environmental conditions favorable to each specific taxon's utilization of phagotrophy. These findings substantially increase our understanding of how *in situ* mixotrophic abundance and proportion are influenced by the planktonic community composition in combination with environmental factors.

Biotic and Abiotic Factors Associated with Temporal and Spatial Variability of Constitutive Mixotroph Abundance and Proportion

Introduction

The classic characterization of pelagic protists separates them into either phytoplankton or zooplankton. However, some protists are categorized as mixotrophs - organisms that combine the use of photosynthesis and prey ingestion to obtain nutrients. While mixotrophs have historically been regarded as a relatively unique and uncommon type of protist, it is now accepted that mixotrophs exist across most major planktonic taxonomic groups, except for diatoms, and they can comprise a substantial proportion of the plankton community (Flynn et al., 2013; Stoecker et al., 2017). Unfortunately, in field studies, mixotrophs are still often misclassified within the phytoplankton and zooplankton dichotomy due to limitations of current methods to accurately identify mixotrophs *in situ* (Flynn et al., 2013; Millette et al., 2018). Mixotrophs are typically grouped with phytoplankton due to the use of photopigments (chlorophyll *a*) as an indicator of photosynthetic capability. However, mixotrophs can also be grouped with zooplankton due to their ability to ingest prey. These misclassifications have led to a lack of data on mixotroph presence and abundance and inadequate representation of mixotrophs in models (e.g. biogeochemical cycling models, food web models). Research needs to transition towards studying mixotrophs as their own group, apart from phytoplankton and zooplankton, in order to understand their unique role in aquatic food webs and ecosystems (Millette et al., 2018). However, to accomplish this, mixotrophs need to first be clearly distinguished from phytoplankton and zooplankton.

Due to the high functional diversity among mixotrophs, multiple functional groups of mixotrophs have been defined based on diversity in their utilization of both nutrient acquisition modes, phototrophy and phagotrophy (Mitra et al., 2016). The major distinction between the different classifications of mixotrophs is based on whether they have their own chloroplast for

photosynthesis or if they utilize (steal) chloroplasts acquired from their prey (Fig. 1; Mitra et al., 2016). Constitutive mixotrophs (CM) have the innate ability to photosynthesize (synthesize and maintain their own chloroplasts), while non-constitutive mixotrophs (NCMs) acquire the ability to photosynthesize by ingesting phototrophic prey (do not constitutively synthesize chloroplasts). From there, NCMs are further divided in two types, generalists non-constitutive mixotrophs (GNCMs) and specialists non-constitutive mixotrophs (SNCMs). GNCMs can acquire chloroplasts from a broad range of phototrophic prey, while SNCMs acquire chloroplasts from specific phototrophic prey (Mitra et al. 2016). Finally, SNCMs can then be divided into mixotrophs that retain only the chloroplasts from their prey, or plastidic (pSNCMs), and mixotrophs that retain the entire photosynthetic prey, or endosymbiotic (eSNCMs).

When studying mixotrophs it is important to understand what mixotrophic group(s) are being targeted (CMs, NCMs, etc.) because it is expected that each mixotrophic functional group will respond differently to environmental changes (Flynn et al., 2013). For my research, I will be focusing on CMs that ingest bacteria because that is what my methods exclusively targets. CMs are ubiquitously important and potentially the most abundant mixotrophic group, capable of ingestion of prokaryotic and eukaryotic prey (Faure et al., 2019; Mitra et al. 2023). However, evidence suggests that a large proportion of CMs are capable of ingesting heterotrophic bacteria (Mitra et al. 2023). This suggests that my study potentially captures the largest proportion of mixotrophs. Previous research has hypothesized that CMs are favored over strict autotrophs when either inorganic nutrients or irradiance levels are limiting for growth, as they can use prey ingestion to acquire the limiting growth factor (Arenovski et al., 1995; Jones et al., 2009; Stoecker, 1998). For example, a study using cultures of the mixotrophic species *Ochromonas minima* (chrysophyte) from Norwegian coastal waters demonstrated that CMs appear to

outcompete strict autotrophs under light limitation or nutrient limitation due to their acquisition of nutrients and energy through prey ingestion (Fischer, 2017). Studies done in the Sargasso Sea and the coastal waters of Norway observed that the relative abundance of CMs was higher in the surface waters (>50%) compared to in the deeper portion of the euphotic zone (barely detectable, Arenovski et al., 1995; Nygaard & Tobiesen, 1993). Those studies attributed the decrease in CMs abundance with increasing depth due to greater availability of dissolved nutrients at depth, which would favor strict autotrophs better adapted for growth at low light intensity. Furthermore, Berge et at. (2017) used a theoretical model to argue that CMs can achieve higher abundances when light and prey are relatively abundant, but nutrients are limited. In all these studies, CMs have an advantage over strict photoautotrophs when only one growth factor is limiting. However, when more than one growth factor is limiting strict heterotrophs have an advantage over CMs (Stoecker, 1998). Other than environmental conditions, factors such as community composition might influence mixotroph abundance. A more recent study by Millette et al. (2021) suggested that dinoflagellate or cryptophyte abundance, depending upon the location, were related to mixotroph abundance.

Alternatively, it is predicted that NCMs have an advantage over strict autotrophs under high light and low prey conditions in oligotrophic systems, as they are dependent on the presence of prey but can supplement missing carbon by photosynthesis through acquired phototrophy from their photoautotrophic prey (Hansen et al., 2013). This means that the competitive advantage of NCMs likely relies on prey densities. NCMs would have an advantage over strict heterotrophs, in prey limiting conditions under both high and low light conditions. Under high light conditions, NCMs may be able to obtain carbon by taking advantage of the photosynthetic capacity acquired from their prey, while under low light conditions, the decrease of

photosynthesis rate may be offset by an increase of grazing rate (Ghyoot et al., 2017; Skovgaard, 1998).

Despite the research efforts conducted so far on mixotrophs, there is still very limited understanding about *in situ* conditions that favor mixotroph activity and abundance. It is necessary to better understand under what conditions mixotrophs are an important factor in the plankton food web because of their role in carbon transport and sequestration (Larsson et al., 2022). Recent studies using theoretical food web models have shown that mixotrophs could potentially increase the transfer of carbon to higher trophic levels (Mitra et al., 2014; Ward and Follows, 2016). However, this work is theoretical, and their model outputs are not ground-truthed by observations and measurements, making it difficult to comprehend where mixotrophs and mixotrophy are an important part of the food web. In this study, I used emerging methods to generate a list of CMs grazing on bacteria in the York River, more accurately estimated the abundance and proportion of CMs by only detecting taxa actively grazing in a given sample, and investigated factors that favor a high proportion and abundance of CMs. This project substantially increases our understanding of the importance of studying mixotrophic protists as a group and how their *in situ* abundance and proportion are potentially influenced by not only environmental factors, but also by the planktonic community composition.

References

Arenovski, A. L., Lim, E. L., Caron, D. A. (1995). Mixotrophic nanoplankton in oligotrophic surface waters of the Sargasso Sea may employ phagotrophy to obtain major nutrients. Journal of Plankton Research. 17: 4, 801–820.

Berge, T., et al. (2017). Modeling succession of key resource-harvesting traits of mixotrophic plankton. ISME J. 11, 212–223.

Fischer, R., et al. (2017). Importance of mixotrophic bacterivory can be predicted by light and loss rates. Oikos. 126, 713–722.

Flynn, K. J., et al. (2013). Misuse of the phytoplankton−zooplankton dichotomy: the need to assign organisms as mixotrophs within plankton functional types. J Plankton Res 35: 3−11.

Ghyoot, C., et al. (2017). Modeling plankton mixotrophy: A mechanistic model consistent with the shutter-type biochemical approach. Front Ecol Evol. 5, 78.

Hansen, P. J., et al. (2013). Acquired phototrophy in *Mesodinium* and *Dinophysis*– a review of cellular organization, prey selectivity, nutrient uptake and bioenergetics. *Harm. Algae.* 28, 126–139.

Jones, R.I. (2000). Mixotrophy in planktonic protists: an overview. Freshw Biol. 45, 219−226.

Jones, H., et al. (2009). Experiments on mixotrophic protists and catastrophic darkness. *Astrobiology* 9, 563–571.

Larsson, M. E, et al. (2022). Mucospheres produced by a mixotrophic protist impact ocean carbon cycling. Nature Communications. 13, 1301.

Millette, N. C., et al. (2018). Hidden in plain sight: The importance of cryptic interactions in marine plankton. Limnol. Oceanogr. Lett. **3**: 341–356. doi:10.1002/lol2.10084.

Millette, N. C., et al. (2021). Temporal and spatial variability of phytoplankton and mixotrophs in a temperate estuary. Mar Ecol Prog Ser. 677, 17-31.

Mitra, A., et al. (2014). The role of mixotrophic protists in the biological carbon pump. *Biogeosciences* 11, 1–11.

Mitra, A., et al. (2016). Defining planktonic protist functional groups on mechanisms for energy and nutrient acquisition: incorporation of diverse mixotrophic strategies. Protist 167:106−120

Nygaard, K., and Tobiesen, A. (1993). Bacterivory in algae: a survival strategy during nutrient limitation. *Limnol. Oceanogr.* 38, 273–279.

Skovgaard, A. (1998). Role of chloroplast retention in a marine dinoflagellate. *Aquat. Microb. Ecol.* 15, 293–301.

Stoecker, D. K. (1998). Conceptual models of mixotrophy in planktonic protists and some ecological and evolutionary implications. Europ. J. Protistol. 34, 281- 290.

Stoecker, D. K., et al. (2017). Mixotrophy in the Marine Plankton. Annu. Rev. Mar. Sci. **9**: 311–335. doi:10.1146/annurev-marine-010816-060617

Ward, B. A., and Follows, M. J. (2016). Marine mixotrophy increases trophic transfer efficiency, mean organism size, and vertical carbon flux. Proc Natl Acad Sci USA. 113, 2958−2963.

Tables and Figures

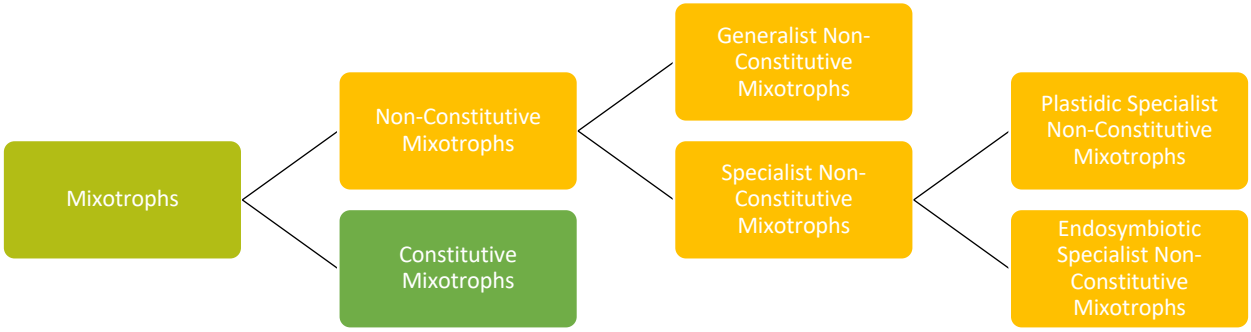

Figure I1. Schematic representation of functional types of mixotrophs. Based on definitions in Mitra et al. 2016.

Chapter 1: Biotic and abiotic factors associated with temporal and spatial variability of constitutive mixotroph abundance and proportion

Introduction

The existence of mixotrophic plankton (organisms that combine photoautotrophy and phagotrophy) has long been recognized. However, it has only been within the past decade that scientists have appreciated that mixotrophs can comprise a substantial portion of the plankton community (Stoecker et al., 2017). The traditional definition of mixotrophs refers to an organism that combines autotrophy and heterotrophy, and when this term is applied to plankton the use of heterotrophy can refer to osmotrophy and phagotrophy. However, it has been argued that since the use of osmotrophy does not differentiate planktonic mixotrophs from prokaryotic and eukaryotic phytoplankton, defining mixotrophic plankton as the use of photoautotrophy and phagotrophy is more useful (Flynn et al., 2013).

There is presently a major gap in our ability to accurately distinguish between phytoplankton, zooplankton, and mixotrophs in field studies, which often leads to the underestimation of mixotroph abundance (Millette et al. 2018). This makes it difficult to understand the relative importance of mixotrophs compared to phytoplankton and zooplankton across spatial and temporal gradients. Mixotrophs are typically grouped with phytoplankton due to the use of photopigments (chlorophyll *a*) as an indicator of photosynthetic capability. However, mixotrophs can also be grouped with zooplankton due to their ability to ingest prey. Given how prevalent mixotrophs can be in the plankton community (Millette et al., 2021; Gilbert and Mitra, 2022), research needs to transition towards studying mixotrophs as their own plankton group(s), apart from phytoplankton and zooplankton, in order to understand their trophic role in aquatic food webs and ecosystems (Flynn et al., 2013; Millette et al., 2018). However, to

accomplish this, mixotrophs need to first be clearly distinguished from phytoplankton and zooplankton so that their abundance can be more accurately estimated.

The ability to estimate *in situ* mixotroph abundance has been hindered by the limitations of current popular methods (Anderson et al., 2017; Li et al., 2021). Mixotroph abundance is typically estimated through the use of fluorescently labeled bacteria or fluorescent microspheres (Anderson et al., 2017; Arenovski et al., 1995; Czypionka et al., 2011; Gast et al., 2018; Millette et al., 2017; Sanders et al., 2000; Sato et al., 2017). These methods work by estimating the *in situ* abundance of cells that consume fluorescently-labeled material and contain chloroplasts (González, 1999). However, it has been demonstrated that these methods chronically *underestimate* mixotroph abundance (Anderson et al. 2017; Li et al., 2021) because these experiments have a short incubation period (<2 hrs) that likely does not capture all grazing activity. Furthermore, certain species might be biased against fluorescently labeled particles, while others may be overly biased towards them (Sanders and Gast, 2012; Wilken et al., 2019). More recently, studies have attempted to estimate mixotroph abundance in publicly available microscopy datasets via taxonomy (Haraguchi et al., 2018; Leles et al., 2019; Cesar-Ribeiro et al., 2020; Schneider et al., 2020; Mitra et al. 2023). This type of analysis uses available microscopy-based taxonomic data to estimate the abundance and proportion of potential mixotrophs (plankton that have been found to be capable of photoautotrophy and phagotrophy in previous peer-reviewed studies) over large temporal and spatial scales. However, this method is likely an *overestimation* of the presence of mixotrophs, since it is not known if a species is actually utilizing mixotrophy in any given sample or location.

It is important to accurately estimate mixotroph abundance because their role in carbon transport and sequestration is expected to be distinct from phytoplankton and zooplankton

(Larsson et al., 2022). Previous research has hypothesized that mixotrophs have an advantage over phytoplankton and zooplankton when either inorganic nutrients or irradiance levels are limiting for growth, as they can use prey ingestion to acquire the limiting growth factor (Arenovski et al., 1995; Jones et al., 2009; Stoecker, 1998). Studies using theoretical food web models have shown that mixotrophs could potentially increase the transfer of carbon to higher trophic levels (Mitra et al. 2014; Ward and Follows, 2016). Therefore, knowledge of the spatial and temporal distribution of mixotroph abundance, and the environmental factors associated with their variability, are crucial for understanding the conditions under which mixotrophs are an important part of the plankton food web.

A relatively new molecular method has been developed to identify active mixotroph species (taxa identified to be grazing when the sample was collected) in field samples. This method involves feeding live bacteria labeled with 5-bromo-2′-deoxyuridine (BrdU), a thymidine analog, to planktonic protists in a natural water sample. Active mixotrophs are identified as taxa that contain chloroplasts and have incorporated BrdU into their DNA (Fay et al., 2013). Then, active mixotrophs identified from the BrdU experiments can be matched with taxa identified in microscopy samples to estimate the abundance and proportion of mixotrophs (Millette et al., 2021). In its current form, the BrdU method targets constitutive mixotrophs (CMs), mixotrophs that actively synthesize and maintain their own chloroplast (Ghyoot et al., 2017), that are ingesting heterotrophic bacteria. CMs are an important type of mixotroph distributed in a wide range of conditions in all waters of the global ocean (Faure et al., 2019). Using this method, the accuracy of what is identified as a CM in microscopy samples (typically species 10-20 µm and larger) increases, as the identification of CMs in microscopy data can be constrained to CMs that are actively grazing in a collected sample. Accurate estimates of *in situ* CM abundance are

necessary to improve our analyses of how CMs vary spatially and temporally in response to environmental conditions and taxa present in the community.

A recent study by Millette et al. (2021) utilized this new molecular method to identify and quantify active CMs and potential CMs in their microscopy samples. However, BrdU experiments were only conducted for six of the twenty-three sample dates, so most of their conclusive results were based on potential CM abundance (taxa that have demonstrated the ability to consume bacteria in their studied system), rather than which taxa were actively grazing in each sample. By conducting BrdU experiments for only a few sample dates, this study included CMs that may not have been actively grazing when most samples were collected, likely still overestimating CM abundance and proportion. For example, they reported that active CMs accounted for 0 - 65% of the phototrophic community counted through microscopy, but potential CMs accounted for 5 – 75% of the phototrophic community over the same six sample dates. Occasional use of the BrdU method can provide information on the CMs present in a specific system, but not necessarily when certain CMs are ingesting bacteria (aka actively engaging in mixotrophy). Using BrdU incubations for all sampling dates can provide a constraint on estimates of CM abundance by identifying taxa actively grazing in each sample, thereby more accurately estimating CM abundance.

The BrdU method has the potential to address a major research gap by more accurately estimating *in situ* CM abundance and proportion in microscopy samples by detecting taxa actively grazing in a given sample. Here, BrdU experiments and microscopy were used to taxonomically identify and assess the variability of CMs that ingest bacteria within a temperate estuary across a whole year. The goal was to apply higher sampling frequency use of the BrdU method in order to investigate the biotic and abiotic factors associated with the temporal and

spatial variability of CMs identifiable though microscopy. To accomplish this goal, I had three objectives: (1) to develop two separate lists of CMs grazing on bacteria in two distinct parts of the York River Estuary, Chesapeake Bay, USA (2) compare the estimations of potential versus active CM abundance and proportion and (3) use the active CM data to investigate the biotic and abiotic factors associated with the spatial and temporal variability of CM abundance and proportion. For my first objective, I hypothesized that the list of CMs grazing on bacteria would be distinct at each specific location, as the presence of taxon with mixotrophic capability does not necessarily mean it is actively grazing. For my second objective, I hypothesized that my estimations of potential CM abundance and proportion would be significantly higher than estimations of active CM abundance and proportion. This would suggest that measurements of potential CM abundance might lead to overestimations of CM abundance, while utilizing the BrdU experiments to identify active CMs might provide a more nuanced estimation of CM abundance by only detecting taxa actively grazing in a given sample. For my third objective, I hypothesized that CMs would have a higher proportional abundance under high light and low nutrient conditions or under low light and high nutrient conditions, but would have lowest proportional abundance under high light and high nutrient conditions. Previous research has suggested that CMs have an advantage over strict autotrophs and strict heterotrophs when either light or nutrients are limiting, but not both (Stoecker, 1998; Edwards, 2019). This study demonstrates that CM abundance might not be only regulated by environmental conditions favorable to mixotrophy but, instead, environmental conditions favorable to each specific taxon's utilization of phagotrophy.

Methodology

Stations

Two stations were sampled twice a month over one year in the York River Estuary, Chesapeake Bay, USA; West Point (WP) and Gloucester Point (GP; Fig. 1). WP is located up-estuary, near one of the two major freshwater sources to the York River (Mattaponi River) at the West Point fishing pier and GP is located closer to the mouth of the estuary at the Gloucester Point fishing pier. The WP station is characterized by low salinities (oligohaline) with high nutrient concentrations and high turbidity, as it is located near the estuarine turbidity maximum (ETM) (Friedrichs, 2009; Reay, 2009). The GP station is situated in a lower turbidity, high salinity zone (meso- to polyhaline) with low nutrient concentrations compared to WP (Friedrichs, 2009; Reay, 2009). The WP station is also usually less stratified than the GP station due to shallower depths and stronger currents, although presence of stratification a GP can oscillate weekly due to the spring-neap tidal cycle (Friedrichs, 2009).

Environmental data

All sampling occurred on an incoming tide, no later than 1 hour before high tide starting at WP. A YSI EXO1 sonde (Xylem Inc.) was used to conduct a vertical profile of temperature (ºC), salinity, and turbidity (FNU: Formazin Nephelometric Unit). The data points for each profile were averaged for every 0.1 m. A LI-1400 (2π quantum sensors; Deck: LI-190SA and Water: LI-192SA) from LI-COR was used to conduct an irradiance profile of the water column and calculate the light attenuation coefficient (k_d) at 0.5m.

A 5 L Niskin bottle (General Oceanics) was used to collect water from just below the surface. Water for nutrient analysis (15mL of 0.45 µm-filtered water) was collected in two 20 mL acid-washed plastic vials. Once in the laboratory, no more than two hours after samples were collected, the nutrient samples were frozen at -20 ºC until analysis for ammonia (NH_3), nitrate + nitrite (NO_x), phosphate (PO_4^{3-}), and silica (SiO_2) (µM) using a Skalar Auto Analyzer in the

Virginia Institute of Marine Science Analytical Services Center (EPA, 1993; EPA, 1997). Water for chlorophyll a analysis was collected in three 1 L clear Nalgene bottles. The bottles were kept in a dark cooler until they were brought back to the laboratory. To measure chlorophyll *a* concentrations, 40-150 mL of the water collected was filtered onto 25 mm GF/Fs. The filters were resuspended in 7 mL of 90% acetone for 24 hours and placed in the freezer at -20 ºC. After 24 hours, the samples were read on a Turner Designs 10-AU fluorometer for chlorophyll *a* concentrations before and after acidification with 10% HCl (Arar & Collins, 1997).

Microscopy

Additional water from the 5 L Niskin cast was collected in three 500 mL Nalgene amber bottles, immediately preserved with 5% Lugol's solution, and sealed with electrical tape. The Lugol's samples were concentrated in the laboratory by settling for 24 hours in a 500 mL beaker and then gently pipetting liquid off the top to reduce the total volume to approximately 50 mL. Chloroplast containing plankton genera/species in these samples were identified and enumerated (cells mL^{-1}) with a Zeiss Axio Imager.A2 microscope at 400x magnification on a Sedgewick rafter slide (Sherr & Sherr, 1993). A minimum of 300 cells were counted per sample.

BrdU-labeled bacterial ingestion experiments

In order to identify active CMs present at each station on each sampling date, incubation experiments were conducted using BrdU labeled bacteria as prey. Two cultures of *Photobacterium angustum* (heterotrophic bacteria) were grown in yeast extract 10 days before sampling. BrdU (800 µM final concentration) was then added to one of the bacterial cultures (+BrdU) three days before sampling (Millette et al., 2021). The BrdU was washed off the culture the day before sampling by centrifuging at 3,000 rpm for 10 min at 4 ºC. The supernatant was removed without disturbing the bacterial pellet. 10 mL of sterile 1x phosphate-buffered saline

(PBS) was used to resuspend pellets and they were centrifuged again. This was repeated three times and after the final wash, bacterial pellets were resuspended in a total of 20 mL sterile 1X PBS and cell concentration determined using hemocytometer. The bacterial culture without BrdU (-BrdU) was also "washed" three times to ensure both cultures were treated the same. The water collected from the Niskin cast was used to set up triplicate incubations for +BrdU and -BrdU bacterial additions. 250 mL of water was placed into a 250 mL clear Nalgene bottle and bacteria was added to a final concentration of 10^6 cells mL^{-1}. The bottles were then incubated for 24 hours in mesh bags in the York River Estuary, near the Virginia Institute of Marine Science. At the end of the experiment, all water from each incubation bottle was collected onto 47 mm 3 µm Isopore filters. Samples were stored in -20 ºC freezer until analyzed.

Immunoprecipitation of +BrdU DNA and sequence analysis

DNA was extracted for all samples following the hot detergent method reported by Gast et al. (2004) using 200 µL of lysis buffer. DNA extracted from +BrdU incubations then went through an immunoprecipitation process that isolated sequences that had incorporated the BrdU into their DNA. The first step in the immunoprecipitation process involved preparing two solutions (antibody mix and dynabeads mix) that were blocked (prevent non-specific binding) using denatured bacterial DNA. This was accomplished by denaturing 300 ng of *P. angustum* DNA per sample (stock of DNA at 30 ng per ul;10 ul per reaction) for 10 min at 95 ºC. The tubes were transferred to an ice bath for 2 min, then cold PBS-BSA (acetylated bovine serum albumin (BSA), 500 mg, BioWorld 22070000-1; used 1mg BSA/mL1x PBS) was added to bring to final volume (30 µL per reaction).

The denatured bacterial DNA was then used to block the anti-BrdU B44 mouse antibodies (BD Biosciences 347580). The denatured bacterial DNA was mixed with same

volume of anti-BrdU mouse antibody (1/10 dilution: 2.5ng.μL^{-1}; 10 µL each for each reaction) in a 1.5 mL microfuge tube and incubated at 4ºC on a rotating mixer for 1 hour (antibody mix). BrdU-labeled DNA samples from the experiments (dilution of 300 ng in 10uL) were denatured at 95ºC for 10 min, placed on ice for 2 minutes, and then 10 µL of cold PBS-BSA was added. Each denatured BrdU DNA sample was then combined with 20 µL of the blocked antibody mix. Next, magnetic dynabeads beads were blocked using the denatured bacterial DNA. Dynabeads M-280 Sheep anti-mouse magnetic beads (Invitrogen 11201D, 20 µL per reaction [decreased by half, diluted with 10µL of PBS-BSA]) were mixed with the same volume of denatured bacterial DNA (dynabeads mix). Then, the antibody mix with the denatured BrdU DNA and the dynabeads mix were incubated overnight at 4 ºC on a rotating mixer. This step allowed for BrdU-labeled DNA to bind to the anti-BrdU mouse antibody and for the dynabeads to be blocked by the denatured bacterial DNA. The following day, blocked dynabeads were vortexed, 40 µL of blocked dynabeads added to each antibody sample and incubated for at least 1 hour at 4 ºC on rotating mixer. This allows for the anti-BrdU mouse antibody that has attached to the BrdU labeled DNA to bind to the dynabeads so that the BrdU-labeled DNA can be magnetically separated.

To remove the DNA that was not BrdU labeled from the beads, tubes were transferred to a magnet (DynaMag^{TM}-2, Invitrogen 12321D) and given about 5 minutes for the dynabeads to attach to the side of the tube. Once it was clear, the solution in the tubes was then removed and discarded. The beads were fully resuspended in 1 mL of washing buffer (PBS with 0.05% Tween 20), then the solution allowed to clear on the magnet, followed by removal of liquid without bead pellet disruption. This step was repeated three times. Then the beads were resuspended in 0.5 mL of washing buffer, the solution allowed to clear on the magnet, followed by removal of liquid without bead pellet disruption. This step was repeated four times for a total of seven washes. To

remove BrdU-labeled DNA from the beads, 100 µL of elution buffer (5mM BrdU in PBS; Sigma B9285-250mg) was added to each sample and incubated at 65 ºC for 20 min. Each sample was then incubated at room temperature for 15 min. Next, the solution was allowed to clear on the magnet and the liquid transferred to a new tube. An ethanol precipitation overnight was done to recover the DNA (90 µL 100% isopropanol, 35 µL 3M NaCl, 100 µL elution). Next day, precipitation reactions were centrifuged (14,000 rpm for 10 min), the liquid carefully removed, and the DNA pellet allowed to dry for several minutes before resuspending the remaining DNA in 10 µL PCR water. The -BrdU DNA collected onto the 47 mm 3 µm Isopore filters did not go through the immunoprecipitation process as only unlabeled bacteria was added to those samples.

Amplicons for -BrdU DNA and immunoprecipitated +BrdU DNA were generated through PCR amplification of the V4 region of the 18S ribosomal gene using primers V418SF (5' [TCGTCGGCAGCGTCAGATGTGTATAAGAGACAG] CCAGCASCYGCGGTAATTCC) and V418SR (5' [GTCTCGTGGGCTCGGAGATGTGTATAAGAGACAG] ACTTTCGTTCTTGATYRATGA), described in Piredda et al. (2017) and modified to include 5' adapter sequences (in square brackets) for Illumina MiSeq. Each sample was amplified in triplicates using up to 3 µL template DNA, 1.25 units GoTaq Flexi DNA polymerase, 2 mM $MgCl_2$, 2 µL 2.5 µM dNTPs, and 2.5 µL 10X reaction buffer (25 µL total volume) with the conditions: 95 ºC for 8 minutes; 35 cycles of 95 ºC for 30 seconds, 58 ºC for 30 seconds, 72 ºC for 90 seconds; 72 ºC for 5 minutes; 4 ºC hold. Some samples were diluted in order to be amplified (Table A2). Amplicons were sent to the Rhode Island Institutional Development Award (IDeA) Network of Biomedical Research Excellence Molecular Informatics Core for library preparation and Illumina MiSeq (300 bp paired end; 600 cycle kit V2) sequencing.

QIIME2 was used to demultiplex, denoise, remove chimeras, and quality control the Illumina data. Amplicon sequence variants (ASVs) were grouped at 100% identity and taxonomy assigned using the Silva 132 database. ASVs identified as bacteria, metazoa, fungi, and macroalgae were removed from the analyzed dataset, as were those that occurred only once (singletons). For each experiment, taxa were identified as bacterivores based on comparison of tag sequences between +BrdU and −BrdU samples. ASV abundances were converted to a percentage of the total tags for each sample, and the average of each −BrdU ASV was subtracted from the average of the corresponding +BrdU ASV. An ASV was considered a bacterivore if the subtracted value was positive and >0.1% of the average total amplicon abundance. Bacterivores identified as taxa containing chloroplasts were then considered actively grazing CMs (Fay et al., 2013; Millette et al., 2021). The use of 0.1% as a cutoff was to represent the more abundant amplicons in the datasets (Millette et al., 2021). This balanced the effect of variability between incubation replicates and reduced the influence of non-specific recovery of extremely abundant DNA (e.g. from diatoms).

Potential and active CM abundance and proportion

The abundance of potential CMs was calculated by adding up the abundance of genera present in each microscopy sample that had been identified as a CM in the BrdU experiments for any sampling date at a specific location. This calculation reflects the abundance of plankton with the ability to engage in mixotrophy but not whether they were actively ingesting bacteria prey, or using their alternate nutrient mode, as done in Millette et al. 2021. To calculate active CM abundance, the CM ASV taxonomic identifications were compared to the microscopically identified taxa, and a qualitative identification of a microscopic taxon as an active CM was made if there were matches at the genus level for each sampling date at each station. This calculation

reflects the abundance of CMs that were actively engaging in mixotrophy at the time the sample was collected. The proportion of potential and active CMs were calculated by dividing the total abundance of taxa identified as either a potential or active CM by the total phototroph abundance for that sample. Potential CM abundance and proportion was compared to active CM abundance and proportion to assess potential overestimations in the presence of CMs when not accounting for which taxa are actively ingesting. Further analysis on biotic and abiotic factors associated with the abundance and proportion of CMs was was only done on active CMs.

Analysis

To examine environmental conditions associated with the proportion of active CMs, and the abundance of diatoms, dinoflagellates, cryptophytes, haptophytes, and active CMs, analyses using poisson generalized linear models with an offset (GLMs) were conducted for both stations. Triplicate samples were kept separate and sample dates with any missing data were removed from analysis (WP: n = 57, GP: n = 48). The independent variables (environmental data) included were temperature, salinity, turbidity, attenuation coefficient (K_d), and nutrient concentrations (NO_x, NH_3, PO_4^{3-}, and SiO_2). The offset term was the proportion of the microscope slide that was counted for each sample. The independent variables for each model run were tested for collinearity using the 'car' package in R with the variance inflation factor (VIF) function (Fox & Weisberg, 2016). Any environmental variable that had a collinearity VIF value of 5 or greater (Zuur et al., 2010) was removed so that analyses were run only with independent variables that were not strongly related to each other. Any variables in the selected GLM with p-values greater than 0.05 were also removed until the final GLM for each dependent variable at a station had only significant variables with no collinearity. All GLM runs were conducted in R (version 3.6.3) using the built-in linear regression (glm) function.

Results

Environmental data

The physical data collected from March 2021 to February 2022 were significantly different between WP and GP (Table 1). The average turbidity, temperature, and K_d were significantly higher at WP (Table 1). The average salinity was significantly higher at GP. However, the majority of biological (chlorophyll *a* concentrations) and chemical (nutrient concentrations) data were not different between WP and GP (Table 1). The only exception to this was NO_x concentrations, which were significantly higher at WP compared to GP (Table 1). Chlorophyll *a* and turbidity were also more variable at WP than GP.

Phototroph abundance and major taxonomic groups

The average (±SE) phototroph abundance (phytoplankton + mixotrophs) was not significantly different between WP (3777 ± 305 cells mL^{-1}) and GP (4883 ± 367 cells mL^{-1}, p-value >0.05, t-test, Fig. 2). However, there were times of the year when phototroph abundance was substantially different between stations. The highest phototroph abundances at WP occurred during the late summer, during the months of August and September, and were still high during September through November (Fig. 2). At GP, phototroph abundances were highest during the winter, in the months of January and February due to a diatom bloom dominated by *Skeletonema* spp. (Fig. 2). The proportion of major taxa groups present between stations and sampling dates was highly variable, but diatoms, dinoflagellates, and cryptophytes were the most dominant taxa groups at both stations (Fig. 3). At WP, dinoflagellates were the most prominent during the spring, while diatoms dominated during the summer, cryptophytes dominated during the autumn, and diatoms dominated again during winter (Fig. 3a). At GP, dinoflagellates dominated in early spring, diatoms dominated during the summer, cryptophytes became the most prominent during

the autumn, and there was a shift towards diatoms dominating again during the winter due to the aforementioned *Skeletonema* spp. bloom (Fig. 3b).

Based on results from GLM analysis, at WP, diatom abundance was positively related to temperature, NH_3 and SiO_2, and negatively related to turbidity, NO_x, PO_4^{3-}, and K_d (Table 2). Dinoflagellate abundance was positively related to temperature, NH_3, and K_d, and negatively related to turbidity, NO_x, and SiO_2 (Table 2). Cryptophyte abundance was positively related to temperature, NH_3, and SiO_2, and negatively related to PO_4^{3-} and K_d (Table 2). Haptophyte abundance was positively related to temperature, NO_x, PO_4^{3-}, and K_d, and negatively related to NH_3 (Table 2). At GP, diatom abundance was positively related to salinity, SiO_2, and K_d, and was negatively related to temperature, NH_3, NO_x, and PO_4^{3-} (Table 3). Dinoflagellate abundance was positively related to temperature and K_d, and was negatively related to salinity, NH_3, NO_x, PO_4^{3-}, and SiO_2 (Table 3). Cryptophyte abundance was positively related to salinity, NH_3, and K_d, and was negatively related to temperature, NO_x, and PO_4^{3-} (Table 3). Haptophyte abundance was positively related to K_d, and was negatively related to temperature, salinity, NH_3, NO_x, PO_4^{3-}, and SiO_2 (Table 3).

Mixotrophic ASVs

A total of one hundred and fifty-nine unique ASVs were identified as containing plastids and associated with BrdU-labeled bacterial ingestion (CMs) over the twenty-four sampling dates between WP and GP. 80% of these ASVs were identified to at least the genus level. Out of the mixotrophic ASVs identified, sixty-three were unique to WP, thirty-four were unique to GP, and sixty-two occurred at both stations. Dinoflagellates ASVs made up the largest proportion (~42%) of all major taxa groups and were the most evenly distributed between the two stations. From the sixty-seven dinoflagellate ASVs identified, thirty-three occurred at both stations, while sixteen

were unique to WP and eighteen were unique to GP. Chrysophytes and cryptophytes were the least evenly distributed between stations. Twenty chrysophyte and thirteen cryptophyte ASVs were unique to WP, while only one chrysophyte and two cryptophyte ASVs were unique to GP. At GP, dinoflagellates comprised over 50% of the ASVs (Fig. 4). At WP, there was more diversity within the mixotrophic ASVs, with chrysophytes (19%), cryptophytes (17%), and dinoflagellates (39%) all accounting for a high proportion of ASVs (Fig. 4).

At both stations, the number of CM ASVs identified for a sampling date was highest in early spring. There was a decrease during the summer and a small increase during the autumn (Fig. 5). Dinoflagellate ASVs were the dominant mixotrophic taxa group throughout the whole year at GP. However, at WP, dinoflagellate ASVs dominated in the first half of the year with cryptophytes becoming dominant later in the year (Fig. 4). Chrysophyte ASVs were always prominent at WP, but never dominant.

Twenty-two of the ASVs could be matched with six genera identified in microscopy samples: *Gymnodinium* spp. (*G. aureolum*, *G. nolleri*, *G. dorsalisulcum*, *G. palustre*, *G.* sp. GSSW10, *G.* uncultured eukaryote, *G.* uncultured marine eukaryote), *Gyrodinium* spp. (*Gyrodinium* uncultured eukaryote, *G. instriatum*, *Gyrodinium* uncultured alveolate, *Gyrodinium* uncultured dinoflagellate, *Gyrodinium* uncultured marine eukaryote), *Heterocapsa* spp. (*H. rotundata*, *H. niei*, *H. triquetra, Heterocapsa* uncultured dinoflagellate, *Heterocapsa* uncultured eukaryote*), Karlodinium* sp. (*Karlodinium* uncultured marine dinoflagellate), *Scrippsiella* spp. (*Scrippsiella* sp. NY012, *Scrippsiella* uncultured marine alveolate), and *Teleaulax* spp. (*Teleaulax* uncultured eukaryote, *Teleaulax* uncultured marine eukaryote) (Fig. 6). The remaining one hundred and thirty-seven ASVs that were identified from the BrdU experiments were not associated with taxa from the microscopy samples. Most of those taxa were either too

small to be accurately identified through microscopy, or were ASVs with general (or non-specific) identification (e.g. chrysophyceae uncultured eukaryote, dinophyceae uncultured eukaryote, cryptophyceae uncultured freshwater eukaryote). It is also possible that a number of these taxa were too rare within the system to captured via light microscopy. Error also could have occurred due to inaccurate taxon identifications via microscopy.

Potential and active CM abundance and proportion

At WP, the average abundance (±SE) of potential CMs was 1221 ± 132 cells mL^{-1} (Fig. 7a), which accounted for 40% ± 3.6 of the average total number of phototrophic cells counted (Fig. 7c). At GP, the average abundance of active CMs was 1387 ± 151 cells mL^{-1} (Fig. 7a), which accounted for 44% ± 2.6 of the average proportion of total phototrophic cells counted (Fig. 7c). The abundance and proportion of potential CMs was highly variable throughout the year at both the GP (376 – 2824 cells mL^{-1}; 4 – 74%) and WP (419 – 3422 cells mL^{-1}; 12 – 83%) stations. The abundance (up to 2824 cells mL^{-1}) and proportion of phototrophic cells that were potential CMs (up to 74%) at GP was highest during spring and autumn, while at WP, abundance (up to 3422 cells mL^{-1}) and proportion of phototrophic cells that were potential CMs (up to 83%) was highest during the spring and winter.

At WP, the average abundance (±SE) of active CMs was 388 ± 56 cells mL^{-1} (Fig. 7b), which accounted for 13% ± 1.6 of the average total number of phototrophic cells counted (Fig. 7d). At GP, the average abundance of active CMs was 274 ± 41 cells mL^{-1} (Fig. 7b), which accounted for 7% ± 0.7 of the average proportion of total phototrophic cells counted (Fig. 7d). The abundance and proportion of active CMs was highly variable throughout the year at both the GP (0 – 1297 cells mL^{-1}; 0 – 38%) and WP (0 – 1270 cells mL^{-1}; 0 – 40%) stations. The abundance (up to 1297 cells mL^{-1}) and proportion of phototrophic cells that were active CMs (up

to 38%) at GP was highest during summer, while at WP, abundance (up to 1270 cells mL^{-1}) and proportion of phototrophic cells that were active CMs (up to 40%) was highest during the autumn and winter.

Cryptophytes and dinoflagellates were the only two taxonomic groups represented in the potential and active CM abundance. For the potential CM abundance calculations, all genera/species classified as CMs through BrdU experiments at each station were included for each sample date. However, the genera/species classified as an active CM in the microscopy samples varied throughout the year and between stations. At WP, there was seasonal variability in the dominant taxonomic group representing active CMs (Fig. 6a). During the spring, dinoflagellates such as *Gymnodinium* spp., *H. rotundata,* and *Scrippsiella* spp. dominated the community of active CMs (Fig. 6a). The cryptophyte *Teleaulax* spp. was more frequently identified as an active CM throughout the autumn (Fig. 6a). While at GP, dinoflagellate ASVs such as *Gymnodinium* spp. and *H. rotundata* were frequently identified as active CMs throughout the whole year in microscopy samples (Fig. 6b).

Based on the GLM analysis, the abundance of active CMs at WP was positively related to temperature, turbidity, NH_3, and SiO_2 concentrations, and negatively related to PO_4^{3-} concentrations and K_d (Table 2). The proportion of active CMs was positively related to NH_3, and SiO_2 concentrations, and negatively related to temperature and K_d (Table 2). The abundance of active CMs at GP was positively related to K_d, and negatively related to temperature, NH_3, NO_x, and PO_4^{3-} concentrations (Table 3). The proportion of active CMs was positively related to K_d, and negatively related to salinity, NH_3, NO_x, and PO_4^{3-} concentrations (Table 3).

Discussion

I utilized a recently developed molecular method to taxonomically identify over one hundred and fifty CMs that ingest bacteria within an estuarine system across one year. These results demonstrate that estimations of CM abundance were ~75% higher for potential CMs compared to active CMs. This suggests that utilizing the BrdU experiments to identify active CMs provides a potentially more nuanced estimation of abundance by only detecting taxa actively grazing in a given sample. Using the active CM abundances, I was able to further demonstrate that the abundance and proportion of active CMs was highest during the autumn at WP and summer at GP. The combination of molecular methods and microscopy allowed me to assess an array of biotic and abiotic factors associated with temporal and spatial variability of CMs. Specifically, I was able, for the first time, to assess how the actively grazing mixotrophic taxa changes throughout the year and potentially impacts CM abundance.

Potential versus active CMs analysis

Measurements of potential CM abundance was 37% higher at GP and 27% higher at WP, compared to the abundance of active CMs. The primary reason for this was because of the continued presence of the cryptophyte *Teleaulax* spp. throughout the whole year at both stations that were only actively grazing at WP during the autumn and rarely ever grazing at GP. This indicates that estimating the abundance of CMs based on who has the capacity to ingest prey overestimates the proportion of the planktonic community that is engaged in mixotrophy in a given sample. Just because a taxon with mixotrophic capability is present, does not necessarily mean it is actively grazing. A recent study also estimated that potential CM abundance and proportion in a temperate estuary (Waquoit Bay, MA, USA), the same way I did in this study (Millette et al. 2021). In Millette's study, dinoflagellates and cryptophytes were also the two taxonomic groups present in the CM abundance calculations, with cryptophytes typically

accounting for the largest proportion of the CM population. However, the results from this study suggest that Millette et al. (2021), may have overestimated the importance of cryptophytes in the CM assemblage and underestimated the importance of dinoflagellates, reinforcing the need to identify actively grazing CMs in microscopy samples as frequently as possible. With enough BrdU experiments, it could be possible to understand the conditions when specific taxa are actively grazing compared to when they are present but not grazing. Understanding environmental factors that trigger grazing in different taxa present in the CM assemblage will be an important target for future research as it will help with the ability to constrain when to consider a species present in microscopy samples as a mixotroph without doing BrdU experiments. Given how different the approaches of estimating potential and active CM abundances are, I did the rest of the analyses focusing only on the active CMs.

Temporal and spatial variability in active CMs

The average water quality data indicated that light and nutrients were significantly different between WP and GP. At WP, light was lower based on higher K_d. At GP, light was higher based on lower K_d. As for nutrient concentrations, NO_x was significantly different between the stations with higher levels at WP. Average PO_4^{3-} and NH_3 concentrations were also higher at WP, although these differences were not significant due to high variability. Overall, this matches up with what is known about the average environmental conditions at these stations, one likely being light limited for phototrophic growth (WP) and the other likely being nutrient limited for phototrophic growth (GP). Given how high K_d was at WP, I assume light was the primary factor limiting photoautotrophic growth. While at GP, given that average NOx concentrations were below 1 µM, I assumed that nutrients were the primary factor limiting photoautotrophic growth. Since both stations have one limiting factor, it was expected that the

importance of CM presence and grazing would be equally important at both stations, albeit for different reasons. Indeed, this is what the CM abundance data displayed with the average abundance and proportion of active CMs not being significantly different between the two stations (Fig. 2). Furthermore, it would be expected that the temporal variability in active CM abundance within each station would vary based on the primary growth limiting factor, light at WP and nutrients at GP. However, results from the GLM analysis suggest that was not the case.

At the WP station, high abundance and proportion of active CMs was associated with high nutrients (high NH_3) and high light (low K_d). This suggests that actively grazing CMs are more prevalent at WP when neither light nor nutrients are limiting. Considering that the upper part of the York River Estuary is known to be light limiting to photoautotrophic growth (Reay, 2009), I would have expected that active CM abundance was negatively related with light levels. At GP, a high abundance and proportion of active CMs was associated with both nutrient (low NH_3^+ and NO_x) and light limitation (low K_d). This suggests that more CMs are actively grazing at GP when both nutrients and light are limiting. Considering that the lower part of the York River Estuary is known to be nutrient limiting to photoautotrophic growth (Reay, 2009), I would have expected that active CM abundance was negatively related with only nutrient concentrations. These results do not align with the hypothesis that CMs have an advantage when only one growth factor is limiting (Stoecker, 1998; Edwards, 2019). Overall, there is evidence that the average environmental conditions between the stations might influence the average abundance of CMs, but factors associated with the variability in active CM abundance at each station might not be entirely tied to environmental conditions. The abundance and proportion of CMs at both stations was correlated to the abundance of major taxonomic groups. At GP, the abundance and proportion of active CMs was correlated to dinoflagellate abundance (*data not*

shown). At WP, while active CM abundance was not correlated with any major taxa group, active CM abundance was correlated with dinoflagellate abundance for the first six months of sampling and cryptophyte abundance for the second six months of sampling (*data not shown*). Dinoflagellates were the dominant mixotrophic ASVs at GP throughout whole year, and dinoflagellates and cryptophytes were the dominant mixotrophic ASVs at WP, depending upon the time of year (Fig. 4). This suggests that when more dinoflagellates are present at GP, and either more dinoflagellates or cryptophytes are present at WP, there will be more active CMs, depending upon the time of year. Furthermore, at GP, the environmental patterns identified to be associated with a high abundance and proportion of CMs using GLM analyses were similar with the patterns associated with a high abundance of dinoflagellates (Table 3). This suggests that the abundance of active CMs is at least partially tied to the taxa present. While, at WP, the GLM results for the abundance and proportion of CMs were similar to the GLM results associated with a high abundance of cryptophytes (Table 2). This challenges the idea that environmental conditions are the only thing, determining active CM abundance. The abundance of active CMs might not be only regulated by environmental conditions favorable to mixotrophy but, instead, environmental conditions favorable to each specific taxon's utilization of phagotrophy.

BrdU method

The BrdU method used in this study is still relatively new, and while it has a lot of potential, it also has drawbacks. First, it is a costly and time-consuming method. The process from adding BrdU to the bacterial cultures, all the way through getting samples ready for sequencing takes around 10 days. The immunoprecipitation process alone takes 3 days of heavily involved and precise work, and only a limited number of samples can be processed at a given time. Depending on the number of samples, the processing of samples could potentially take

months. For all that effort, this method exclusively targets mixotrophs with their own chloroplasts that are ingesting bacteria (constitutive mixotrophs, CM), excluding other types of mixotrophs. However, CMs are an important and ubiquitous mixotrophic group and commonly ingest bacteria (Faure et al., 2019; Mitra et al. 2023). This method might also be biased towards the detection of mixotrophic dinoflagellates relative to other mixotrophic taxa due to their high ribosomal gene copy number (Millette et al., 2021). Although, I detected a substantial number of other mixotrophic ASVs such as chlorophytes, cryptophytes, and chrysophytes. Furthermore, taxa present in high abundances such as diatoms, might lead to non-specific recovery, undermining confidence in other species classified as mixotrophs as diatoms are not mixotrophs (Flynn et al. 2013). Also, I was unable to microscopically identify most of the mixotrophic ASVs, potentially underestimating my abundance of active CMs. However, most of the ASVs not identified in the microscopic samples consisted of taxa that were too small (<10 μm) to be identified and were not included in my reported active CM abundances. Therefore, the active CM abundance data should be considered a representation of CM >10-15 μm.

Although imperfect, this method identifies all the mixotrophic taxa in a sample actively ingesting bacteria. Thus, allowing for the creation of a list of active CMs that ingest bacteria within the environment being studied. This method not only allowed me to identify over one hundred and fifty CMs (80% to the genus level), but also allowed me to create two separate lists of CMs unique to distinct parts of a temperate estuary. By adjusting the sampling frequency or stations, future studies using this method could be expanded to study the time of year or conditions that different CM ASVs are identified to be actively grazing compared to when they are present and not grazing. This would substantially improve our estimations of the abundance and proportion of potential CMs from long-term microscopy-based taxonomic datasets.

Conclusion

This study allowed me to substantially increase our understanding on how *in situ* CM abundance and proportion are influenced by not only environmental factors, but by the taxa present. It is critical to identify CMs that have been misclassified as strict photoautotrophs and the factors favoring their high abundance and proportion as CMs respond differently to changes in biotic and abiotic factors (Stoecker, 1998; Edwards, 2019). I demonstrated that measurements of potential CM abundance showed a substantial overestimation of the presence of CMs when compared to active CM abundance; the presence of mixotrophic taxa in the system does not necessarily mean mixotrophic activity. This highlights the limitations within studies that recategorize phytoplankton from microscopy-based taxonomic datasets to estimate mixotroph abundance, as this study shows that most species were not always grazing when they were present. Analysis with historical datasets are still very useful because they can help rapidly increase our understanding of large-scale mixotrophs presence and distribution, but we need to better constrain the organisms classified as mixotrophs based on the conditions they are grazing under. The BrdU method can be used to help identify the conditions under which CMs are actively grazing, and more accurately use those datasets. This way, we will expand our knowledge on the spatial distribution of CM abundance over large time periods so we can better understand their contribution to aquatic food webs.

Tables and Figures

	Chl *a* ($\mu g\ L^{-1}$)	Sal*	Turb (FNU)*	Temp (°C)*	NH_3 (μM)	NO_x (μM)*	PO_4^{3-} (μM)	SiO_2 (μM)	K_d ($dB\ m^{-1}$)*
WP	18.8±3.5	6.5±0.7	19.4±2.3	18.9±2.1	6.0±1.0	2.3±0.3	0.14±0.02	6.2±0.9	3.8±0.2
GP	13.0±1.6	19.0±0.4	4.8±0.6	18.2±2.0	4.2±0.7	0.4±0.2	0.09±0.03	8.7±1.7	1.5±0.1

Table 1. Average (±SE) water quality data collected 24 times between March 2021 and February 2022 at 2 stations in the York River. Chl *a*: chlorophyll *a*; Sal: salinity; Turb: turbidity; Temp: temperature; NH_3: ammonia concentration; NO_x: nitrate + nitrite concentration; PO_4^{3-}: phosphate concentration; SiO_2: silica concentration; K_d: light attenuation coefficient. *Significant difference between the 2 stations (paired, 2-tailed t-test, $p < 0.05$).

WP	Temp	Turb	NH_3	NO_x	PO_4^{3-}	SiO_2	K_d
Total diatoms	+	-	+	-	-	+	-
Total dinoflagellates	+	-	+	-		-	+
Total cryptophytes	+		+		-	+	-
Total haptophytes	+		-	+	+		+
Active mixotroph abundance	+	+	+		-	+	-
Proportion of active mixotrophs	-		+			+	-

Table 2. Results for the Poisson generalized linear model (GLM) with an offset analysis for select groups at West Point (WP). The factors temperature (Temp), turbidity (Turb), ammonium (NH_3), nitrate + nitrite (NOx), phosphate (PO_4^{3-}), and silica (SiO_2) were used in at least 1 of the models. (−/+): factor was positively (+) or negatively (−) related to the dependent variable. Blank space: factor was not significantly ($p > 0.05$) related to variability in the dependent variable or was removed due to collinearity (VIF > 5).

GP	Temp	Sal	NH_3	NO_x	PO_4	SiO_2	K_d
Total diatoms	-	+	-	-	-	+	+
Total dinoflagellates	+	-	-	-	-	-	+
Total cryptophytes	-	+	+	-	-		+
Total haptophytes	-	-	-	-	-	-	+
Active mixotroph abundance	-		-	-	-		+
Proportion of active mixotrophs		-	-	-	-		+

Table 3. Same as Table 2 but for Gloucester Point (GP).

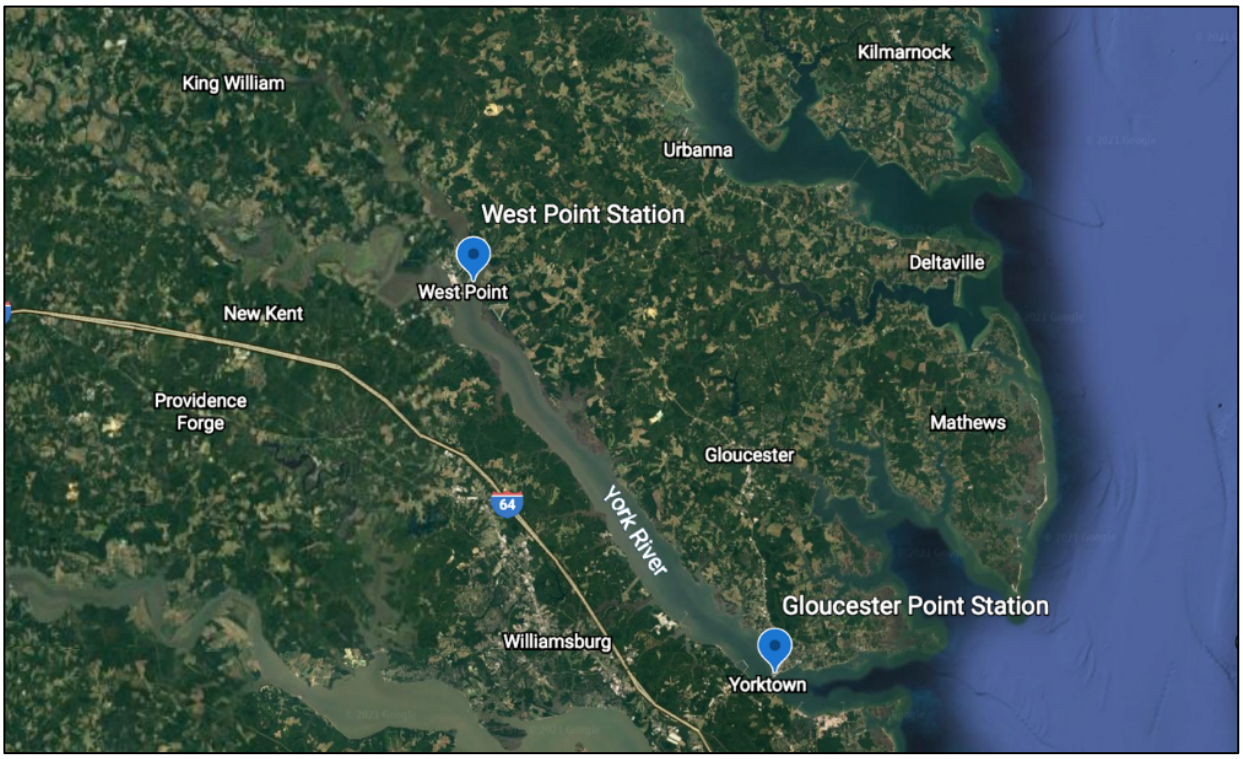

Figure 1. Map of location of fieldwork, with the two different sampling stations across the York River marked with blue dot. West Point Station (WP) – West Point Fishing Pier, and Gloucester Point Station (GP) – Gloucester Point Fishing Pier.

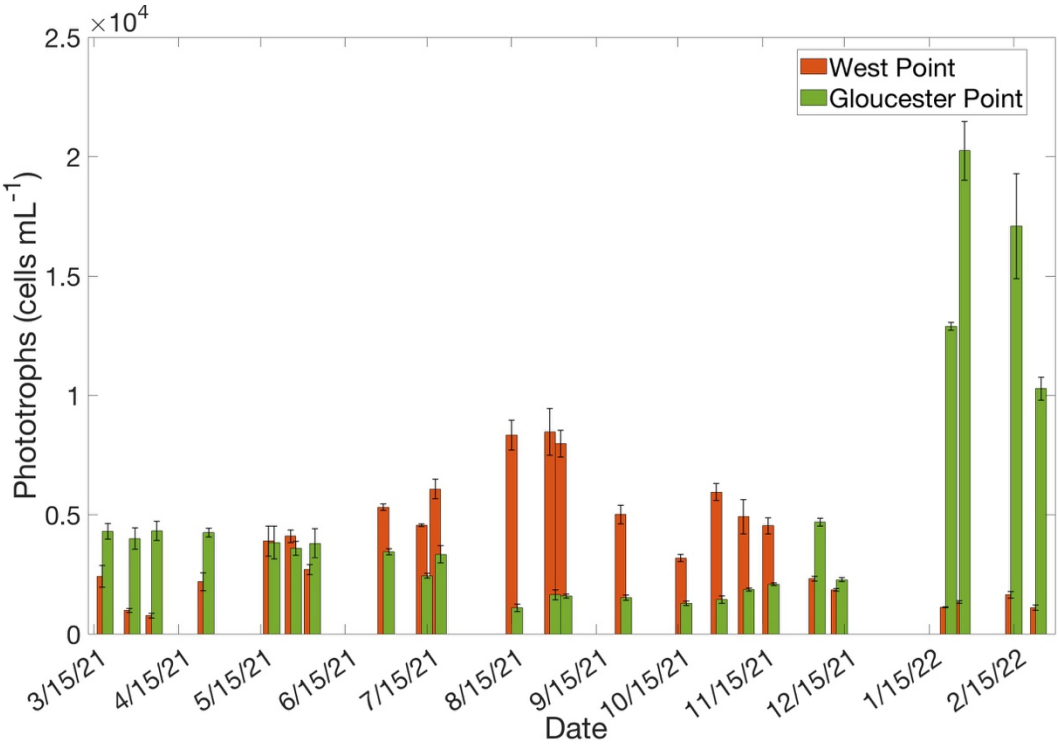

Figure 2. Total abundance of phototrophs (±SE) at WP and GP between March 2021 and February 2022.

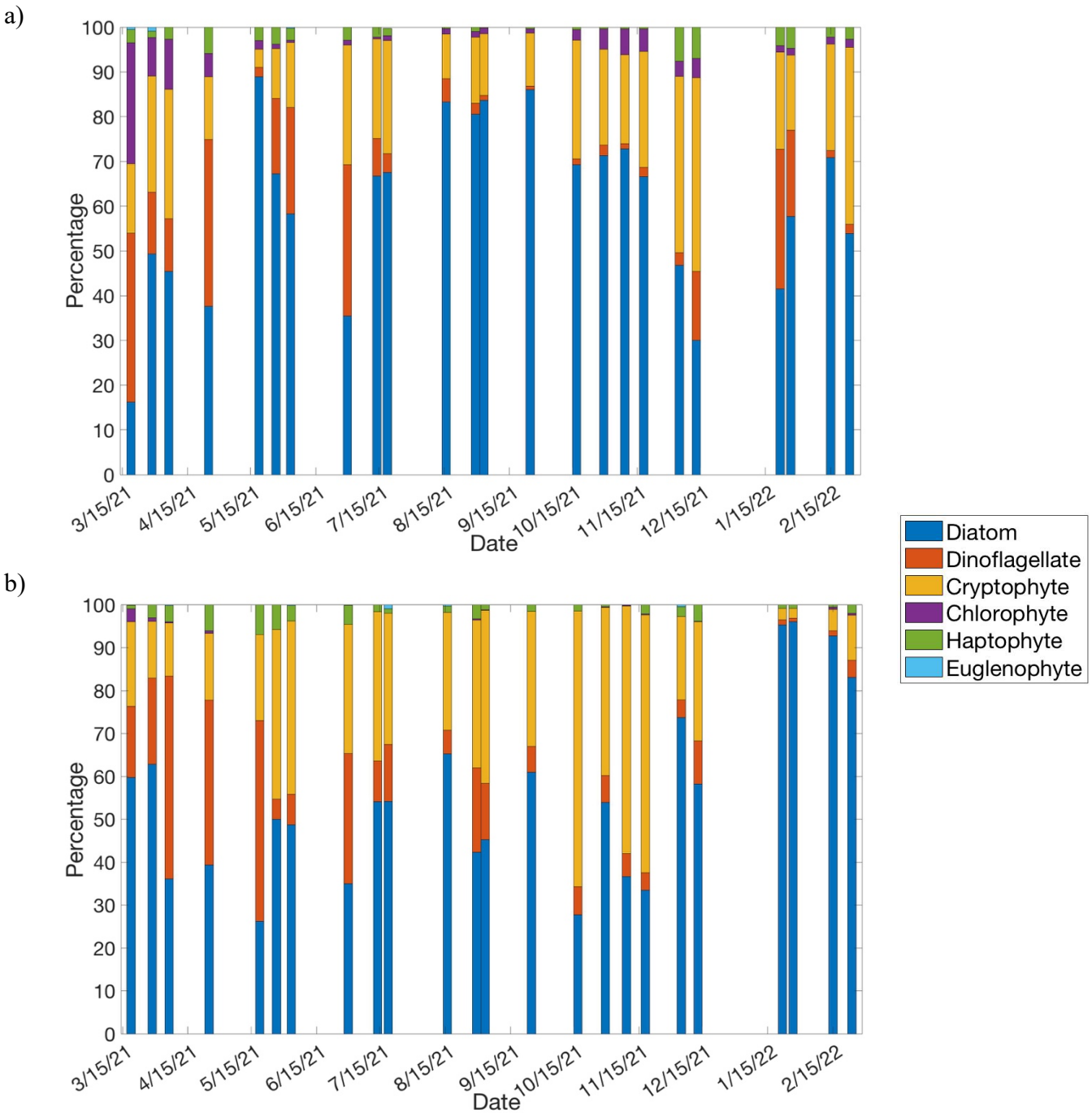

Figure 3. Proportion of total abundance that 6 plankton groups, identified through microscopy, accounted for at each sample date between March 2021 and February 2022 at (a) WP and (b) GP.

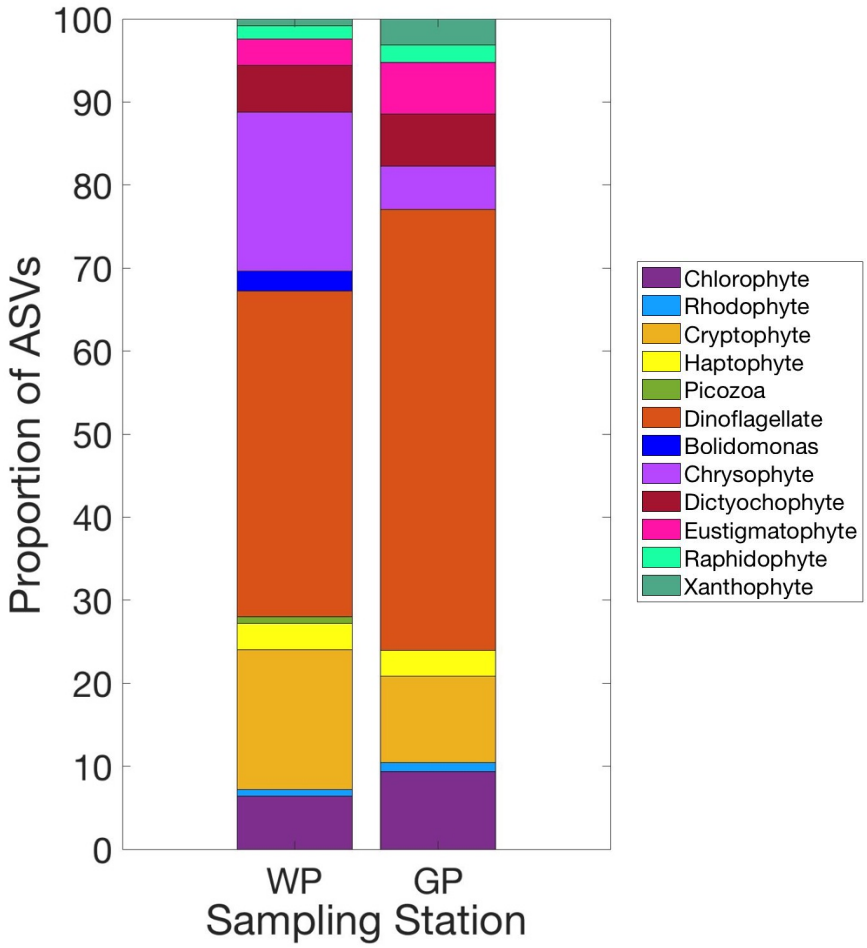

Figure 5. Proportion of mixotrophic ASVs of each major taxonomic group at a) WP and b) GP stations.

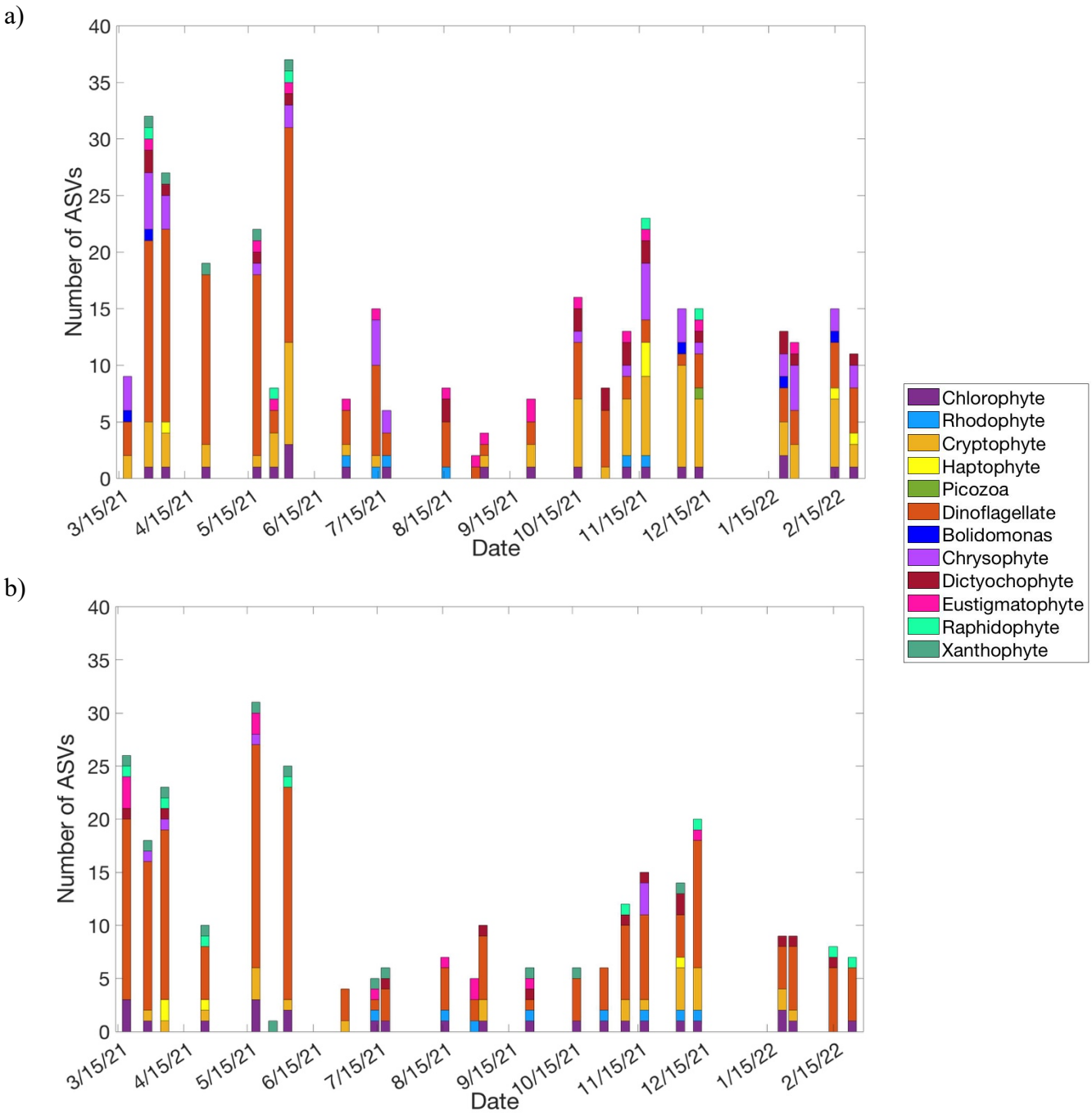

Figure 4. Number of active CMs for each major taxa group identified through Illumina sequencing at WP (a) and GP (b) stations for each sampling date. Each bar corresponds to the number of individual ASVs classified as being a CM based on chloroplast containing sequences that were ingesting BrdU labeled bacteria.

a)

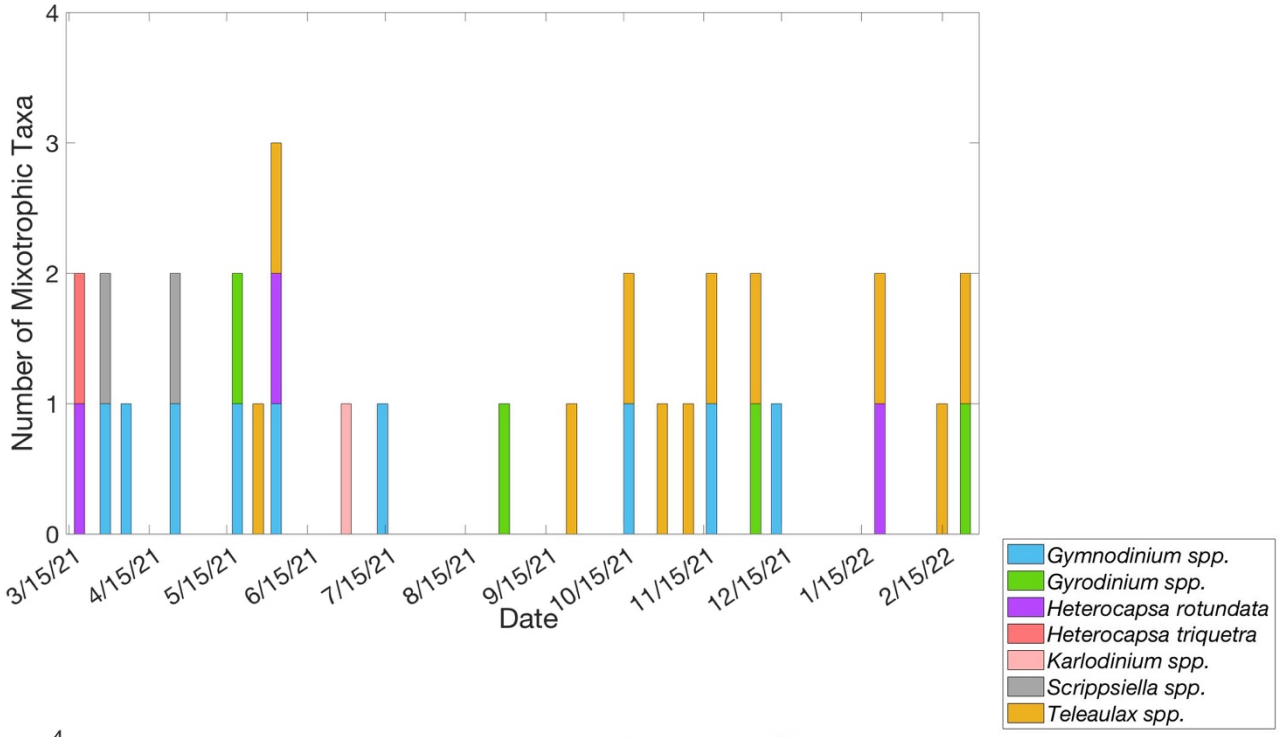

b)

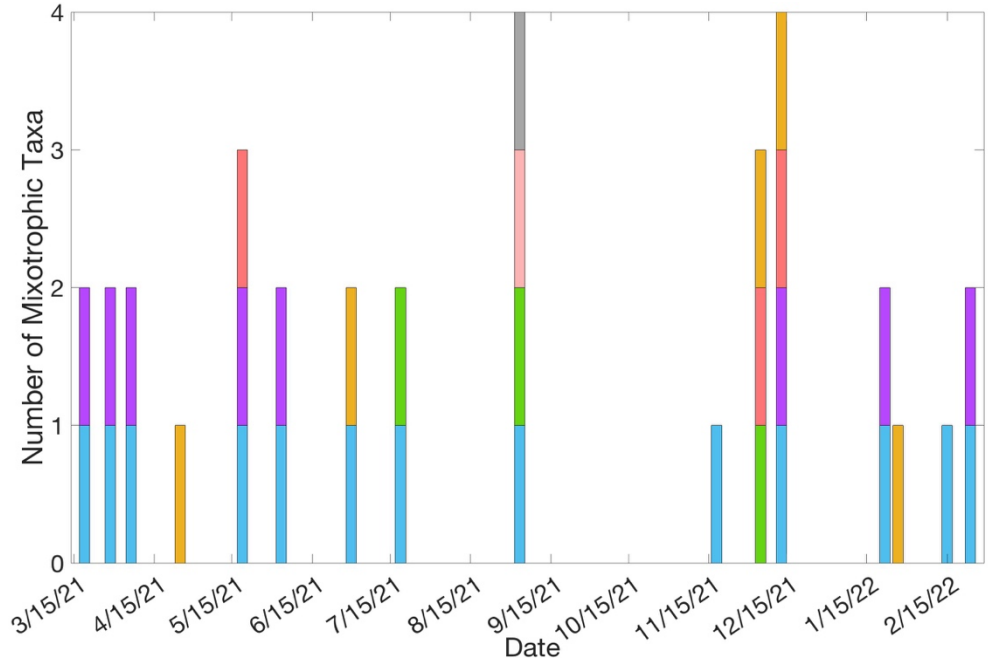

Figure 6. Number of genera/species of each major taxonomic group classified as an active CM in the microscopy samples at a) WP and b) GP stations.

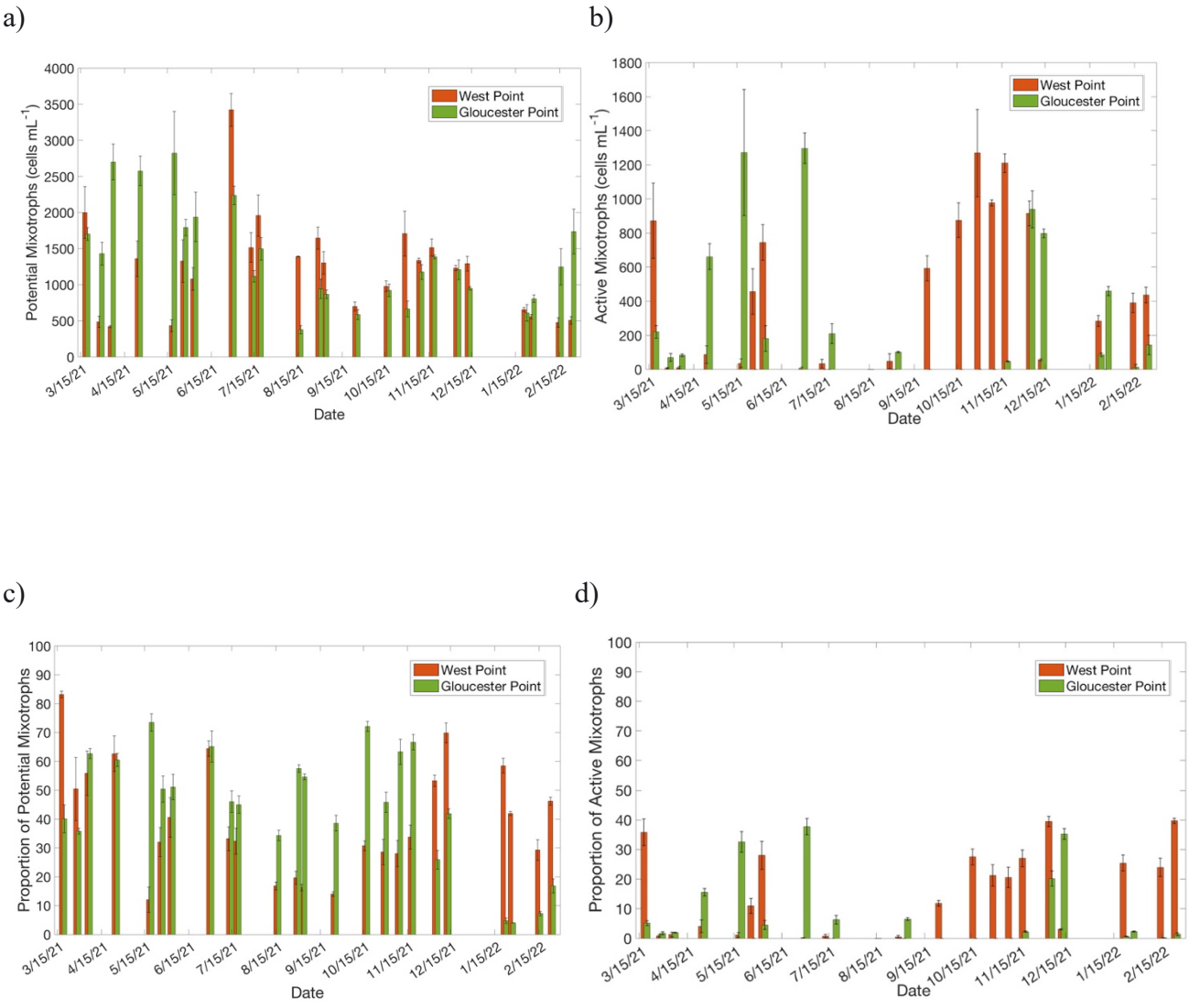

Figure 7. a) Estimated abundance of potential CMs in all microscopy samples based on the genera of chloroplast-containing plankton that have demonstrated the of ingesting bacteria in previous experiments. b) Total abundance of active CMs in microscopy samples identified through the BrdU experiments for each sampling date at WP and GP stations. The active CMs were identified based on the genera/species of chloroplast-containing plankton that were ingesting BrdU labeled bacteria for each sampling date. c) Estimated proportion of potential CMs in all microscopy samples based on the genera of chloroplast-containing plankton that have demonstrated the of ingesting bacteria in previous experiments. d) The proportion of active CMs present at WP and GP stations. The proportional abundance of active CMs was calculated by dividing the abundance of genera/species identified as active CMs by the total abundance of phototrophs of each sampling date.

Future Research

In addition to highlighting the importance of community composition in combination with environmental factors as drivers of mixotroph abundance and proportion, my research exposed a major research gap in the ability to accurately identify *in situ* mixotrophs, with current methods often underestimating or overestimating mixotroph abundance. I suggest several directions for future research that would lead to a better understanding of mixotrophs as a group.

1. *Continue and expand the use of BrdU method combined with microscopy for widespread estimations of mixotroph abundance based on taxonomy of plankton samples*.

   Increasing our knowledge of the spatial and temporal distribution of mixotrophs will help us understand conditions that will favor mixotrophs over strict autotrophs and strict heterotrophs and identify regions where mixotrophs will have a large impact on aquatic environments. By continuing and expanding the use of the BrdU method, the assessment of abundance, distribution, and mixotrophy on a global scale would increase. This would allow for a global perspective of mixotroph biogeography, including the importance of mixotrophs under different community compositions and environmental conditions.

2. *Seasonal patterns and long-term changes in mixotrophic abundance and proportion*.

   Widespread use of BrdU incubations would allow for the development of lists of potential mixotrophs for specific locations. The data can then be matched up with previously collected microscopy and environmental data for those locations. This would give us more robust estimations of mixotroph abundance, and the environmental conditions associated with mixotrophs for those locations around the world. The historical data of phytoplankton species available through taxonomic datasets would

allow us to put observations into a broader temporal context. We would be able to understand if the conditions I sampled are standard, compared to average values for data collected in previous years, seasonally and annually. This would allow us to infer how likely it is that current data on mixotrophic abundance and proportion reflect normal mixotrophic activity at different locations. Furthermore, identifying long-term trends in the dataset will allow us to determine the spatial variability in annual rates of change for mixotrophic abundance and proportion, and for multiple environmental factors.

3. *Analysis of the influence of community composition in mixotroph abundance.*

This research showed how community composition is an important driver of mixotroph abundance and proportion. A thorough analysis of the mixotrophic species present at each location and the environmental conditions associated with their prevalence and when they are actively grazing would increase our understanding of the spatial and temporal variability of mixotroph abundance and proportion.

Appendix

Seasonal patterns in constitutive mixotroph abundance and proportion within the York River

Methods

Historical data of phytoplankton abundance from the Chesapeake Bay Program (CBP) (Michael Lane, personal communication) collected between 1986 to 2020 were analyzed to assess seasonal patterns of CM abundance and proportion. I specifically analyzed data from CBP stations WE4.2 and RET4.3 (Fig. A1) because they were closely located to the two stations sampled throughout the year, GP and WP, respectively. WE4.2 is located by the mouth of the York River, close to the GP sampling station, and RET4.3 is a lower salinity region farther up the river, close to the WP sampling station. CBP samples were collected at least monthly throughout the year but sometimes occurred twice a month during bloom events. However, there are data gaps from missed sampling dates, which mostly occur during the winter. For each sampling date, only a single 15 L composite sample was collected. A portion of that sample (500 mL) was fixed in Lugol's solution and preserved with buffered formalin for phytoplankton analysis. Phytoplankton samples were settled in Utermöhl chambers and enumerated using an inverted microscope. Samples were analyzed to the lowest practical taxonomic level. The CBP dataset includes phytoplankton abundance data for samples collected above and below the pycnocline. For analysis, I focused on data collected above pycnocline layer. The mixotrophic taxa identified through the BrdU experiments were used to determine the CMs present in the CBP dataset. The list of mixotrophic taxa identified in the +BrdU experiments from the WP and GP sampling stations were used to determine the CMs present in the CBP RET4.3 and WE4.2 stations, respectively (Table A2), assuming these taxa were potential CMs throughout the CBP

time series. It is not assumed that these taxa were grazing when the samples were collected, but these potential CMs are taxa that have previously exhibited mixotrophic capability. The proportional abundance of CMs at each station was calculated by dividing the abundance of genera/species identified as CMs by the total phytoplankton abundance of each sampling date. These mixotrophic abundance estimations were referred to as potential CMs because although data on whether these taxa were consuming bacteria when the samples were collected were not available, they have demonstrated the ability to consume bacteria in other York River samples. For this analysis, I was interested in comparing the seasonal variability in CM abundance and proportion between stations. This was accomplished by averaging the total phytoplankton abundance and the abundance of CMs by month for each station. Then, I calculated the average proportional abundance of CMs for each month at each station. Bar plots were created to observe seasonal patterns of CMs abundance and proportion.

Results

Mixotrophic ASVs

At RET4.3, 22 of the WP ASVs could be matched with 11 genera identified in the historical microscopy samples: *Alexandrium* spp. (*A. ostenfeldi*), *Gymnodinium* spp. (*G. aureolum, G. nolleri, G. dorsalisulcum, G.* sp. GSSW10, *G.* uncultured eukaryote), *Gyrodinium* spp.(*Gyrodinium* uncultured alveolate, *Gyrodinium* uncultured dinoflagellate, *Gyrodinium* uncultured eukaryote), *Heterocapsa* spp. (*H. niei*, *H. triquetra, Heterocapsa* uncultured dinoflagellate, *Heterocapsa* uncultured eukaryote), *Polykrikos* spp. (*P. geminatum*), *Scrippsiella* spp. (*S.* sp. *NY012* and *Scrippsiella* uncultured marine alveolate), *Chroomonas* spp. (*C. coerulea* and *Chroomonas* unidentified cryptomonad U53191) , *Cryptomonas* spp., *Apedinella* spp. (*A. radians*), *Dinobryon* spp. (*D. faculiferum*), *Ochromonas* spp. (*O*. sp., *Ochromonas* uncultured

eukaryote). At WE4.2, 25 of the GP ASVs could be matched with 14 genera identified in the historical microscopy samples: *Akashiwo* spp. (*A*. sp. *AP-LIS1*), *Alexandrium* spp. (*A. monilatum*), *Amphidinium* spp. (*A.* sp. *HG114* and *A. steinii*), *Gymnodinium* spp. (*G. dorsalisulcum, G. palustre, G.* sp. *GSSW10*, *G.* uncultured eukaryote, *G.* uncultured marine eukaryote), *Gyrodinium* spp. (*Gyrodinium* uncultured dinoflagellate, *Gyrodinium* uncultured marine eukaryote), *Heterocapsa* spp. (*H. niei*, *H. triquetra, Heterocapsa* uncultured dinoflagellate, *Heterocapsa* uncultured eukaryote), *Katodinium* spp. (*Katodinium* uncultured eukaryote), *Polykrikos*. spp (*P. kofoifii* and *P. geminatum*), *Scrippsiella* spp. (*S.* sp. *NY012), Scenedesmus* spp. (*S.* sp. *KMMCC1258*), *Cryptomonas* spp., *Apedinella* spp. (*A. radians*), *Dinobryon* spp. (*D. faculiferum*), *Ochromonas* spp. (*Ochromonas* sp. *CCMP1278* and *Ochromonas* uncultured eukaryote).

Potential CM abundance and proportion

At RET4.3, the average abundance (±SE) of potential CMs was 2237 ± 1961 cells mL^{-1} (Fig. A2a), which accounted for 23% ± 11 of the average total number of cells counted (Fig. A2b). At WE4.2, the average abundance of potential CMs was 1488 ± 1142 cells mL^{-1} (Fig. A2a), which accounted for 27% ± 11 of the average proportion of total cells counted (Fig.A2b). The abundance and proportion of potential CMs was highly variable throughout the year at both stations. At RET4.3, the abundance of potential CMs (up to 3597 cells mL^{-1}) was highest during spring while the proportion of potential CMs (up to 31%) was highest during winter. At WE4.2 the abundance of potential CMs (up to 2106 cells mL^{-1}) was highest during summer while the proportion of potential CMs (up to 44%) was highest during winter. Dinoflagellates, cryptophytes, chlorophytes, and chrysophytes were the taxonomic groups represented in the potential CM abundance. At both RET4.3 and WE4.2 stations, cryptophytes and dinoflagellates

were the dominating taxonomic groups representing potential CMs throughout the years (Fig. A3).

Discussion

The historical analysis of the CBP phytoplankton abundance data showed significantly higher average abundance and proportion of CMs at RET4.3 (2237 cells mL^{-1}; 23%) and WE4.2 (1488 cells mL^{-1}; 27%) compared to the average abundance and proportion of CMs using my approach at WP (388 cells mL^{-1}; 13%) and GP (274 cells mL^{-1}; 7%). The seasonal patterns associated with CMs dominating the phototrophic community were also different between the historical analysis of the CBP phytoplankton data and my study. At RET4.3, the abundance of CMs was highest during spring compared to the abundance of CMs at WP being highest during autumn. The proportion of CMs at RET4.3 (up to 31%) and WP (up to 40%) were both highest during winter. The abundance of CMs at WE4.2 and GP were both highest during summer. At WE4.2, the proportion of CMs (up to 44%) was highest during winter comparted to the proportion of CMs (up to 38%) at GP being highest during summer. This spatial and temporal variability in the abundance and proportion of potential and active CMs is mostly due to the *overestimation* of the presence of CMs at RET4.3 and WE4.2, as it is not known if a taxon was utilizing mixotrophy when those samples were collected.

Due to the drawbacks associated with estimating potential CM abundance, taxon with mixotrophic capability that were present were always classified as CMs although they may not have been grazing. Looking at the number of genera/species of each major taxonomic group classified as an active CM in the microscopy samples, dinoflagellates were the dominant taxonomic group throughout the whole year at GP, while at WP dinoflagellates dominated in the first half of the year with cryptophytes becoming dominant later in the year (Fig. 6). But, when

you look at potential CMs, cryptophytes were the dominant taxonomic groups throughout the whole year at both the RET4.3 and WE4.2 stations (Fig. A3). In this case when determining the abundance of potential CMs, cryptophytes were always considered as grazing when according to the analyses performed in chapter 1, that was not always true. In chapter 1, there were several times throughout the year at both stations when cryptophytes were present but not actively grazing. Although, in this study the estimations of potential CMs abundance were more nuanced than other studies, as taxa were separately classified as CMs for each station depending on where it was identified ingesting bacteria through the BrdU experiments.

Tables and Figures

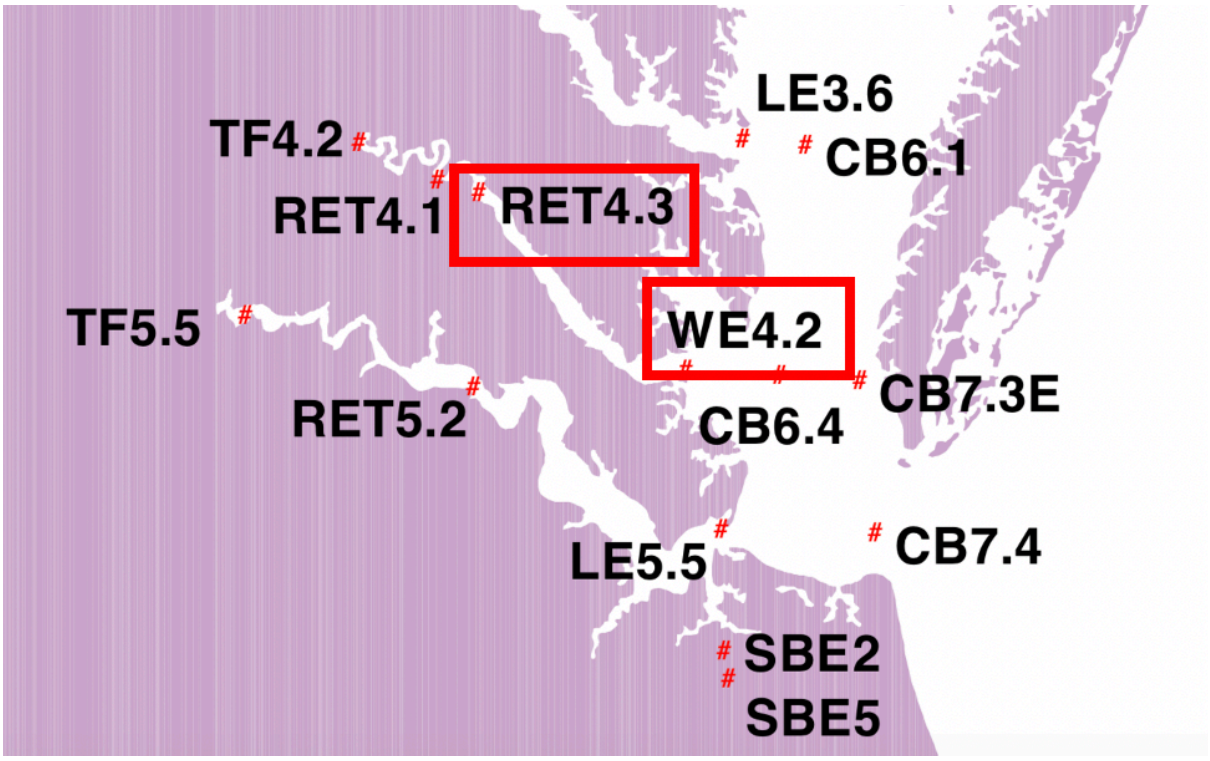

Figure A1. Chesapeake Bay Program map of plankton and vertical fluorescence monitoring stations including stations RET4.3 and WE4.2 highlighted by red box, that was used for historical analyses.

a)

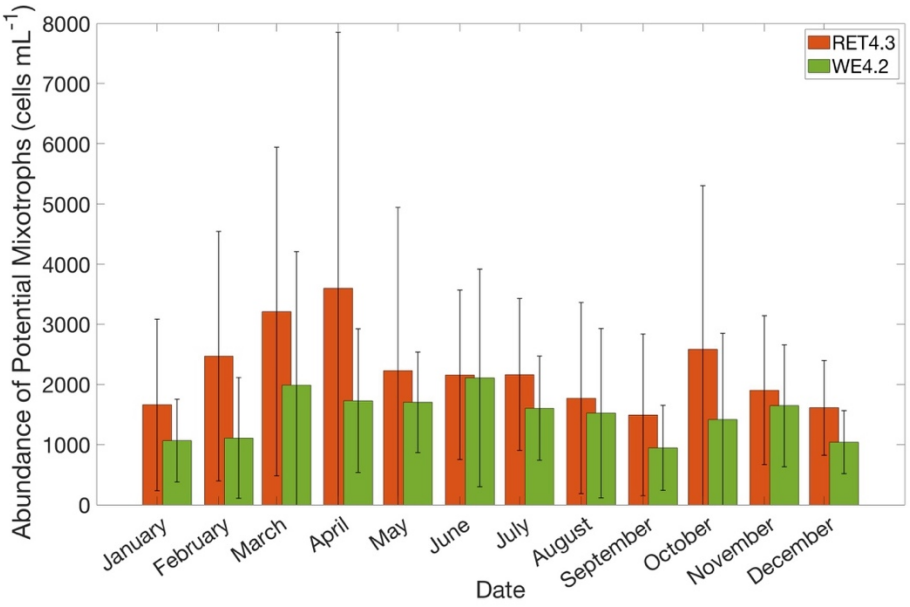

b)

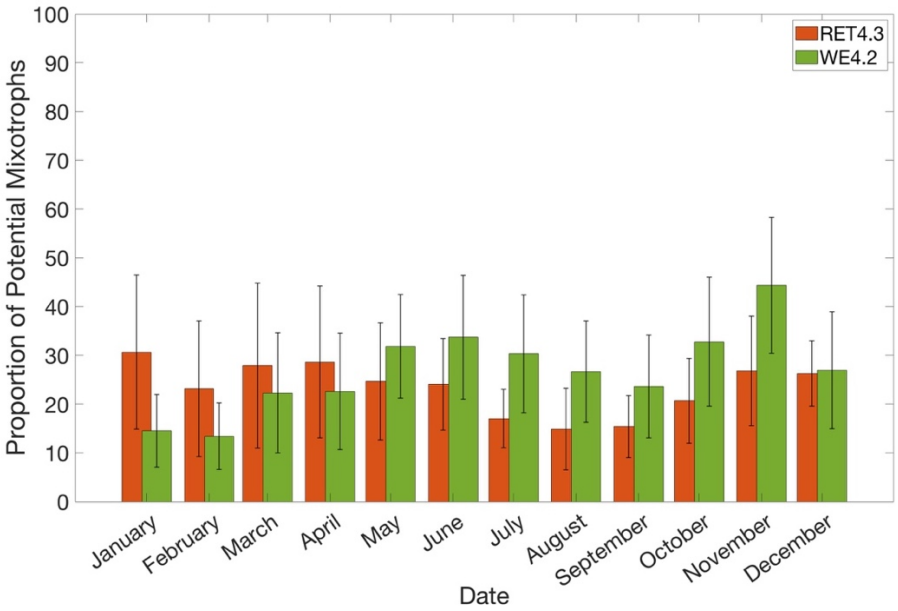

Figure A2. a) Average abundance of potential CMs in historical microscopy samples from 1986-2020 for each month at RET4.3 and WE4.2 stations. Taxa were identified as a potential CM based on the two lists of CMs generated for each station through the BrdU method. b) The proportion of potential CM present at RET4.3 and WE4.2 stations. The proportional abundance of potential CMs was calculated by dividing the abundance of genera/species identified as potential CMs by the total average abundance of each month from 1986-2020.

a)

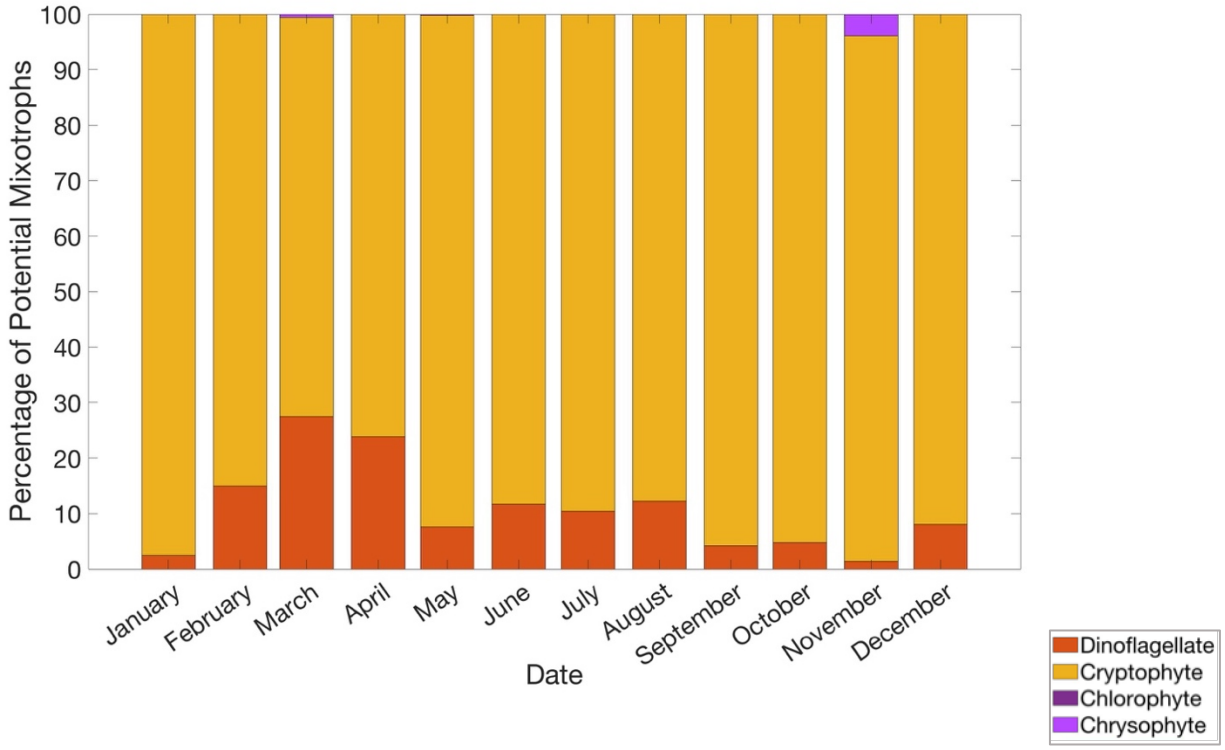

b)

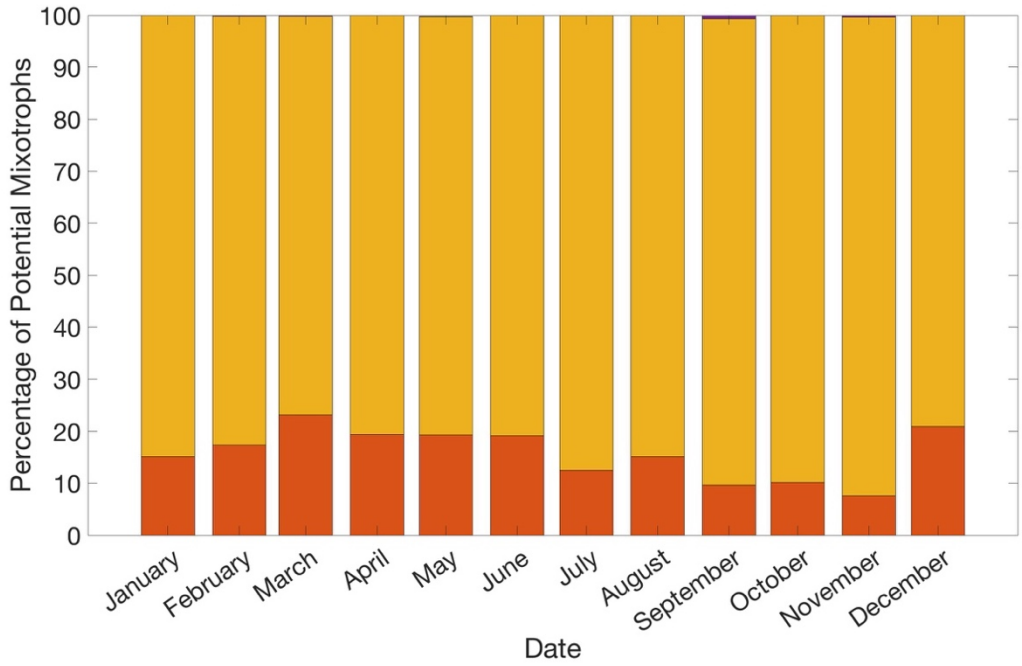

Figure A3. Proportion of estimated potential CMs composed of 4 major taxa groups identified through microscopy at (a) RET4.2 and (b) WE4.2.

ASVs		
GP	WP	BOTH
Scenedesmus sp. KMMCC 1258	*Ostreococcus* uncultured eukaryote	*Ostreococcus* marine metagenome
Monoraphidium contortum	*Ostreococcus* uncultured marine picoeukaryote	*Amphikrikos* sp. J.C.Han 43
Mychonastes jurisii	*Oocystaceae* sp. GSL021	*Porphyridium sordidum*
Ostreococcus tauri	*Oocystaceae* sp. NIES 3919	*Teleaulax* uncultured eukaryote
Proteomonas uncultured eukaryote	*Chroomonas coerulea*	*Teleaulax* uncultured marine eukaryote
Algirosphaera robusta	*Chroomonas* unidentified cryptomonad U53191	*Cryptophyta* sp. CR-MAL11
Amphidinium sp. HG114	*Hemiselmis cryptochromatica*	*Katablepharis* uncultured eukaryote
Amphidinium steinii	*Hemiselmis rufescens*	*Leucocryptos* uncultured eukaryote
Chytriodinium uncultured dinoflagellate	Hemiselmis uncultured alveolate	*Isochrysis galbana*
Gymnodinium palustre	*Cryptophyta* sp. CR-MAL03	*Chrysochromulina* uncultured marine picoeukaryote
Gymnodinium uncultured marine eukaryote	*Rhinomonas nottbecki*	*Sinophysis* uncultured marine eukaryote
Gyrodiniellum uncultured dinoflagellate	*Rhodomonas baltica*	*Gymnodinium dorsalisulcum*
Gymnoxanthella uncultured eukaryote	*Goniomonas aff. amphinema*	*Gymnodinium* sp. GSSW10
Lepidodinium uncultured marine dinoflagellate	*Goniomonas* sp. ATCC 50108	*Gymnodinium* uncultured eukaryote
Pheopolykrikos hartmannii	*Chrysochromulina* uncultured Chrysochromulina	*Lepidodinium* uncultured eukaryote
Polykrikos kofoidii	*Chrysochromulina* uncultured haptophyte	*Paragymnodinium* uncultured eukaryote
Gyrodinium uncultured marine eukaryote	*Dissodinium pseudolunula*	*Polykrikos geminatum*
Akashiwo sp. AP-LIS1	*Gymnodinium aureolum*	*Warnowia* sp. BSL-2009a
Katodinium uncultured eukaryote	*Gymnodinium cf. nolleri*	*Levanderina fissa*
Suessiaceae sp. YY1405	*Paragymnodinium* uncultured marine picoplankton	*Gyrodinium* uncultured dinoflagellate
Suessiaceae sp. mi11-8kt	*Gymnodinium* clade uncultured alveolate	Karenia mikimotoi
Alexandrium monilatum	*Gyrodinium* uncultured alveolate	*Karlodinium* uncultured marine dinoflagellate

Ochromonas sp. CCMP1278	*Gyrodinium* uncultured eukaryote	*Takayama cf. pulchellum*
Ciliophrys infusionum	*Karenia brevis*	*Biecheleria natalensis*
Pedinella uncultured marine eukaryote	*Symbiodinium* uncultured marine plankton	*Biecheleria* uncultured alveolate
Monodus subterranea	*Alexandrium ostenfeldii*	*Biecheleria* uncultured dinoflagellate
Eustigmatophyceae sp. Itas 9/21 S-8w	*Pyxidinopsis* sp. HG-2017a	*Pelagodinium* uncultured eukaryote
Botrydiopsis pyrenoidosa	*Aduncodinium glandula*	*Pelagodinium* uncultured marine dinoflagellate
Chlorellidium tetrabotrys	*Durinskia baltica*	*Protodinium simplex*
Trebouxiophyceae uncultured eukaryote	*Islandinium* uncultured marine eukaryote	*Symbiodinium* uncultured dinoflagellate
Cryptomonadales uncultured eukaryote	*Pfiesteriaceae* sp. CCMP1835	*Amphidiniopsis* uncultured eukaryote
Dinophyceae uncultured freshwater eukaryote	*Scrippsiella* uncultured marine alveolate	*Heterocapsa niei*
Dinoflagellata uncultured dinoflagellate	*Bolidomonas* uncultured eukaryote	*Heterocapsa triquetra*
Eustigmatales uncultured eukaryote	*Bolidomonas* uncultured stramenopile	*Heterocapsa* uncultured dinoflagellate
	Bolidomonas uncultured marine eukaryote	*Heterocapsa* uncultured eukaryote
	Chrysowaernella hieroglyphica	*Scrippsiella* sp. NY012
	Chrysosaccus sp. CCMP295	*Haplozoon* uncultured eukaryote
	Chrysocapsa sp. UTCC280	*Dinobryon faculiferum*
	Uroglena uncultured	*Ochromonas* uncultured eukaryote
	Ochromonas sp.	*Apedinella radians*
	Chromophyton vischeri	*Pseudopedinella* uncultured eukaryote
	Hibberdia magna	*Pteridomonas* uncultured eukaryote
	Paraphysomonas butcheri	*Monodus* sp. NIES-3918
	Paraphysomonas vestita	*Heterosigma akashiwo*
	Paraphysomonas metagenome	Chattonellales MOCH-3 uncultured stramenopile
	Paraphysomonas uncultured chrysophyte	Mamiellophyceae uncultured eukaryote
	Paraphysomonas uncultured eukaryote	Archaeplastida; Chloroplastida
	Paraphysomonas uncultured marine picoeukaryote	

	Mallomonas uncultured Synurales *Spumella* sp. Spumella-like flagellate JBAS36 *Pseudopedinella elastica* *Pedinellales* sp. RCC2286 *Nannochloropsis* uncultured marine eukaryote Cryptomonadales uncultured eukaryote Kathablepharidae uncultured katablepharid Cryptophyceae uncultured freshwater eukaryote Picomonadida uncultured phototrophic eukaryote Chrysophyceae uncultured chrysophyte Chrysophyceae uncultured freshwater eukaryote Chrysophyceae uncultured marine eukaryote Chrysophyceae uncultured stramenopile Chrysophyceae uncultured marine stramenopile Pedinellales uncultured Pedinellales	Cryptomonadales uncultured cryptophyte Cryptomonadales uncultured marine picoeukaryote *Kathablepharidae* uncultured eukaryote *Sinophysis* uncultured dinoflagellate *Suessiaceae* uncultured alveolate *Suessiaceae* uncultured eukaryote Dinophyceae uncultured eukaryote Dinophyceae uncultured marine dinoflagellate *Noctilucales* uncultured eukaryote Chrysophyceae uncultured eukaryote Chrysophyceae uncultured marine picoeukaryote Pedinellales uncultured stramenopile Eustigmatales uncultured phytoplankton Eustigmatales uncultured stramenopile Xanthophyceae uncultured marine eukaryote

Table A1. List of potential mixotrophic ASVs for WP and GP stations based on phototrophic taxa were identified to be grazing at each location through the BrdU incubations.

Vile #	Date	Station	Sample	Dilution Ratio	Vile #	Date	Station	Sample	Dilution Ratio
1	3/19/21	WP	+BrdU	-	149	9/3/21	WP	-BrdU	1:50
2	3/19/21	WP	+BrdU	-	150	9/3/21	WP	-BrdU	1:50
4	3/19/21	WP	-BrdU	1:5	151	9/3/21	GP	+BrdU	-
6	3/19/21	WP	-BrdU	1:5	152	9/3/21	GP	+BrdU	-
7	3/19/21	GP	+BrdU	-	153	9/3/21	GP	+BrdU	-
8	3/19/21	GP	+BrdU	-	154	9/3/21	GP	-BrdU	1:20
9	3/19/21	GP	+BrdU	-	155	9/3/21	GP	-BrdU	1:20
10	3/19/21	GP	-BrdU	-	156	9/3/21	GP	-BrdU	1:20
11	3/19/21	GP	-BrdU	1:50	157	9/25/21	WP	+BrdU	-
12	3/19/21	GP	-BrdU	-	158	9/25/21	WP	+BrdU	-
13	3/29/21	WP	+BrdU	-	159	9/25/21	WP	+BrdU	-
14	3/29/21	WP	+BrdU	-	160	9/25/21	WP	-BrdU	1:20
15	3/29/21	WP	+BrdU	-	161	9/25/21	WP	-BrdU	1:20
16	3/29/21	WP	-BrdU	1:50	162	9/25/21	WP	-BrdU	1:20
17	3/29/21	WP	-BrdU	1:50	163	9/25/21	GP	+BrdU	-
19	3/29/21	GP	+BrdU	-	164	9/25/21	GP	+BrdU	-
21	3/29/21	GP	+BrdU	-	165	9/25/21	GP	+BrdU	-
23	3/29/21	GP	-BrdU	-	166	9/25/21	GP	-BrdU	1:20
24	3/29/21	GP	-BrdU	1:10	167	9/25/21	GP	-BrdU	1:20
25	4/6/21	WP	+BrdU	-	168	9/25/21	GP	-BrdU	1:20
27	4/6/21	WP	+BrdU	-	169	10/17/21	WP	+BrdU	-
28	4/6/21	WP	-BrdU	1:50	170	10/17/21	WP	+BrdU	-
29	4/6/21	WP	-BrdU	1:50	171	10/17/21	WP	+BrdU	-
31	4/6/21	GP	+BrdU	-	172	10/17/21	WP	-BrdU	1:20
32	4/6/21	GP	+BrdU	-	173	10/17/21	WP	-BrdU	1:20
33	4/6/21	GP	+BrdU	-	174	10/17/21	WP	-BrdU	1:20
34	4/6/21	GP	-BrdU	-	175	10/17/21	GP	+BrdU	-
35	4/6/21	GP	-BrdU	-	176	10/17/21	GP	+BrdU	-
36	4/6/21	GP	-BrdU	1:50	177	10/17/21	GP	+BrdU	-
37	4/25/21	WP	+BrdU	-	178	10/17/21	GP	-BrdU	1:20
38	4/25/21	WP	+BrdU	-	179	10/17/21	GP	-BrdU	1:20
39	4/25/21	WP	+BrdU	-	180	10/17/21	GP	-BrdU	1:20
40	4/25/21	WP	-BrdU	1:50	181	10/30/21	WP	+BrdU	-
41	4/25/21	WP	-BrdU	1:50	182	10/30/21	WP	+BrdU	-
42	4/25/21	WP	-BrdU	1:50	183	10/30/21	WP	+BrdU	-
43	4/25/21	GP	+BrdU	-	184	10/30/21	WP	-BrdU	1:20
44	4/25/21	GP	+BrdU	-	185	10/30/21	WP	-BrdU	1:20
45	4/25/21	GP	+BrdU	-	186	10/30/21	WP	-BrdU	1:20
46	4/25/21	GP	-BrdU	1:50	187	10/30/21	GP	+BrdU	-
47	4/25/21	GP	-BrdU	1:50	188	10/30/21	GP	+BrdU	-
48	4/25/21	GP	-BrdU	1:50	189	10/30/21	GP	+BrdU	-
49	5/19/21	WP	+BrdU	-	190	10/30/21	GP	-BrdU	1:20
51	5/19/21	WP	+BrdU	-	191	10/30/21	GP	-BrdU	1:20
52	5/19/21	WP	-BrdU	1:50	192	10/30/21	GP	-BrdU	1:20
53	5/19/21	WP	-BrdU	1:10	193	11/9/21	WP	+BrdU	-
54	5/19/21	WP	-BrdU	1:10	194	11/9/21	WP	+BrdU	-
55	5/19/21	GP	+BrdU	-	195	11/9/21	WP	+BrdU	-

56	5/19/21	GP	+BrdU	-	196	11/9/21	WP	-BrdU	1:20
57	5/19/21	GP	+BrdU	-	197	11/9/21	WP	-BrdU	1:20
58	5/19/21	GP	-BrdU	1:100	198	11/9/21	WP	-BrdU	1:20
59	5/19/21	GP	-BrdU	1:50	199	11/9/21	GP	+BrdU	-
60	5/19/21	GP	-BrdU	1:50	200	11/9/21	GP	+BrdU	-
61	5/27/21	WP	+BrdU	-	201	11/9/21	GP	+BrdU	-
62	5/27/21	WP	+BrdU	-	202	11/9/21	GP	-BrdU	1:20
63	5/27/21	WP	+BrdU	-	203	11/9/21	GP	-BrdU	1:20
64	5/27/21	WP	-BrdU	1:50	204	11/9/21	GP	-BrdU	1:20
65	5/27/21	WP	-BrdU	1:50	205	11/18/21	WP	+BrdU	-
66	5/27/21	WP	-BrdU	1:50	206	11/18/21	WP	+BrdU	-
67	5/27/21	GP	+BrdU	-	207	11/18/21	WP	+BrdU	-
68	5/27/21	GP	+BrdU	-	208	11/18/21	WP	-BrdU	1:20
69	5/27/21	GP	+BrdU	-	209	11/18/21	WP	-BrdU	1:20
70	5/27/21	GP	-BrdU	1:50	210	11/18/21	WP	-BrdU	1:20
71	5/27/21	GP	-BrdU	1:50	211	11/18/21	GP	+BrdU	-
72	5/27/21	GP	-BrdU	1:50	212	11/18/21	GP	+BrdU	-
73	6/3/21	WP	+BrdU	-	213	11/18/21	GP	+BrdU	-
74	6/3/21	WP	+BrdU	-	214	11/18/21	GP	-BrdU	1:20
75	6/3/21	WP	+BrdU	-	215	11/18/21	GP	-BrdU	1:20
76	6/3/21	WP	-BrdU	1:50	216	11/18/21	GP	-BrdU	1:20
77	6/3/21	WP	-BrdU	1:50	217	12/5/21	WP	+BrdU	-
78	6/3/21	WP	-BrdU	-	218	12/5/21	WP	+BrdU	-
79	6/3/21	GP	+BrdU	-	219	12/5/21	WP	+BrdU	-
80	6/3/21	GP	+BrdU	-	220	12/5/21	WP	-BrdU	1:20
81	6/3/21	GP	+BrdU	-	221	12/5/21	WP	-BrdU	1:20
82	6/3/21	GP	-BrdU	1:50	222	12/5/21	WP	-BrdU	1:20
83	6/3/21	GP	-BrdU	1:10	223	12/5/21	GP	+BrdU	-
84	6/3/21	GP	-BrdU	1:50	224	12/5/21	GP	+BrdU	-
85	6/30/21	WP	+BrdU	-	225	12/5/21	GP	+BrdU	-
86	6/30/21	WP	+BrdU	-	226	12/5/21	GP	-BrdU	1:20
87	6/30/21	WP	+BrdU	-	227	12/5/21	GP	-BrdU	1:20
88	6/30/21	WP	-BrdU	1:10	228	12/5/21	GP	-BrdU	1:20
89	6/30/21	WP	-BrdU	1:10	229	12/13/21	WP	+BrdU	-
90	6/30/21	WP	-BrdU	1:10	230	12/13/21	WP	+BrdU	-
91	6/30/21	GP	+BrdU	-	231	12/13/21	WP	+BrdU	-
92	6/30/21	GP	+BrdU	-	232	12/13/21	WP	-BrdU	1:20
93	6/30/21	GP	+BrdU	-	233	12/13/21	WP	-BrdU	1:20
94	6/30/21	GP	-BrdU	1:20	234	12/13/21	WP	-BrdU	1:20
95	6/30/21	GP	-BrdU	1:20	235	12/13/21	GP	+BrdU	-
96	6/30/21	GP	-BrdU	1:20	236	12/13/21	GP	+BrdU	-
97	7/14/21	WP	+BrdU	-	237	12/13/21	GP	+BrdU	-
98	7/14/21	WP	+BrdU	-	238	12/13/21	GP	-BrdU	1:20
99	7/14/21	WP	+BrdU	-	239	12/13/21	GP	-BrdU	1:20
100	7/14/21	WP	-BrdU	1:10	240	12/13/21	GP	-BrdU	1:20
101	7/14/21	WP	-BrdU	1:10	241	1/22/22	WP	+BrdU	-
102	7/14/21	WP	-BrdU	1:10	242	1/22/22	WP	+BrdU	-
103	7/14/21	GP	+BrdU	-	243	1/22/22	WP	+BrdU	-
104	7/14/21	GP	+BrdU	-	244	1/22/22	WP	-BrdU	1:20

105	7/14/21	GP	+BrdU	-	245	1/22/22	WP	-BrdU	1:20
106	7/14/21	GP	-BrdU	1:20	246	1/22/22	WP	-BrdU	1:20
107	7/14/21	GP	-BrdU	1:20	247	1/22/22	GP	+BrdU	-
108	7/14/21	GP	-BrdU	1:20	248	1/22/22	GP	+BrdU	-
109	7/19/21	WP	+BrdU	-	249	1/22/22	GP	+BrdU	-
110	7/19/21	WP	+BrdU	-	250	1/22/22	GP	-BrdU	1:20
111	7/19/21	WP	+BrdU	-	251	1/22/22	GP	-BrdU	1:20
112	7/19/21	WP	-BrdU	1:10	252	1/22/22	GP	-BrdU	1:20
113	7/19/21	WP	-BrdU	1:10	253	1/27/22	WP	+BrdU	-
114	7/19/21	WP	-BrdU	1:20	254	1/27/22	WP	+BrdU	-
115	7/19/21	GP	+BrdU	-	255	1/27/22	WP	+BrdU	-
116	7/19/21	GP	+BrdU	-	256	1/27/22	WP	-BrdU	1:50
117	7/19/21	GP	+BrdU	-	257	1/27/22	WP	-BrdU	1:20
118	7/19/21	GP	-BrdU	1:20	258	1/27/22	WP	-BrdU	1:20
119	7/19/21	GP	-BrdU	1:20	259	1/27/22	GP	+BrdU	-
120	7/19/21	GP	-BrdU	1:20	260	1/27/22	GP	+BrdU	-
121	8/16/21	WP	+BrdU	-	261	1/27/22	GP	+BrdU	-
122	8/16/21	WP	+BrdU	-	262	1/27/22	GP	-BrdU	1:20
123	8/16/21	WP	+BrdU	-	263	1/27/22	GP	-BrdU	1:20
124	8/16/21	WP	-BrdU	1:50	264	1/27/22	GP	-BrdU	1:20
125	8/16/21	WP	-BrdU	1:50	265	2/15/22	WP	+BrdU	-
126	8/16/21	WP	-BrdU	1:50	266	2/15/22	WP	+BrdU	-
127	8/16/21	GP	+BrdU	-	267	2/15/22	WP	+BrdU	-
128	8/16/21	GP	+BrdU	-	268	2/15/22	WP	-BrdU	1:20
129	8/16/21	GP	+BrdU	-	269	2/15/22	WP	-BrdU	1:20
130	8/16/21	GP	-BrdU	1:20	270	2/15/22	WP	-BrdU	1:20
131	8/16/21	GP	-BrdU	1:20	271	2/15/22	GP	+BrdU	-
132	8/16/21	GP	-BrdU	1:20	272	2/15/22	GP	+BrdU	-
133	8/30/21	WP	+BrdU	-	273	2/15/22	GP	+BrdU	-
134	8/30/21	WP	+BrdU	-	274	2/15/22	GP	-BrdU	1:20
135	8/30/21	WP	+BrdU	-	275	2/15/22	GP	-BrdU	1:50
136	8/30/21	WP	-BrdU	1:20	276	2/15/22	GP	-BrdU	1:20
137	8/30/21	WP	-BrdU	1:20	277	2/24/22	WP	+BrdU	-
138	8/30/21	WP	-BrdU	1:20	278	2/24/22	WP	+BrdU	-
139	8/30/21	GP	+BrdU	-	279	2/24/22	WP	+BrdU	-
140	8/30/21	GP	+BrdU	-	280	2/24/22	WP	-BrdU	1:20
141	8/30/21	GP	+BrdU	-	281	2/24/22	WP	-BrdU	1:20
142	8/30/21	GP	-BrdU	1:100	282	2/24/22	WP	-BrdU	1:20
143	8/30/21	GP	-BrdU	1:20	283	2/24/22	GP	+BrdU	-
144	8/30/21	GP	-BrdU	1:20	284	2/24/22	GP	+BrdU	-
145	9/3/21	WP	+BrdU	-	285	2/24/22	GP	+BrdU	-
146	9/3/21	WP	+BrdU	-	286	2/24/22	GP	-BrdU	1:20
147	9/3/21	WP	+BrdU	-	287	2/24/22	GP	-BrdU	1:20
148	9/3/21	WP	-BrdU	1:50	288	2/24/22	GP	-BrdU	1:20

Table A2. Dilution factors for samples amplified. Dashes (-) represent samples that did not need to be diluted for amplification.

Amplicon sequence

These are the basic qiime2 steps that were used to analyze my MiSeq data.

Demultiplex

qiime tools import --type 'SampleData[PairedEndSequencesWithQuality]' --input-path <manifest file name> --output-path <name.qza> --input-format SingleEndFastqManifestPhred33V2

Denoise, dereplicate, quality filter & remove chimeras

qiime dada2 denoise-paired --i-demultiplexed-seqs <.qza file from above> --p-trim-left-f 10 --p-trim-left-r 10 --p-trunc-len-f 290 --p-trunc-len-r 155 --p-max-ee-f 10 --p-max-ee-r 10 --p-chimera-method pooled --o-table <name.qza> --o-representative-sequences <name.qza> --o-denoising-stats <name.qza>

Merge table and repseq files

qiime feature-table merge --i-tables <list tables> --o-merged-table <new table name> qiime feature-table merge-seqs --i-data <list of repset files> --o-merged-data <new file name>

Cluster sequences based upon identity

qiime vsearch cluster-features-de-novo --i-table <name.qza> (table created by dada2) --i-sequences <name.qza> (rep-seqs file created by dada2) --p-perc-identity 1.0 --o-clustered- table <name.qza> --o-clustered-sequences <name.qza>

Remove singletons

qiime feature-table filter-features --i-table <name of table generated in prior step> --p-min-frequency 3 --o-filtered-table <new table name .qza>

qiime feature-table filter-seqs --i-data <name of rep seq file created in prior step> --i-table <name of filtered table> --o-filtered-data <new repseq file .qza>

Assign taxonomy

qiime feature-classifier classify-consensus-vsearch --i-query <name.qza> (this is the rep-set of sequences just created by cluster) --i-reference-reads silva132_99.qza --i-reference- taxonomy taxonomy_all_levels.qza --p-maxaccepts 1 --o-classification <name.qza>

References

Anderson, R., K. Jürgens, and P. J. Hansen. (2017). Mixotrophic phytoflagellate bacterivory field measurements strongly biased by standard approaches: A case study. Front. Microbiol. 8: 1398. doi:10.3389/fmicb.2017.01398.

Arar, E. J., Collins, G. B. (1997). In vitro determination of chlorophyll a and pheophytin a in marine and freshwater algae by fluorescence. Method 445.0, National Exposure Research Laboratory, EPA.

Arenovski, A. L., Lim, E. L., Caron, D. A. (1995). Mixotrophic nanoplankton in oligotrophic surface waters of the Sargasso Sea may employ phagotrophy to obtain major nutrients. Journal of Plankton Research. 17: 4, 801–820.

Cesar-Ribeiro, C., et al. (2020). Is oligotrophy an equalizing factor driving microplankton species functional diversity within Agulhas rings? Front Mar Sci. 7.

Cohen, R. R. H. (1985). Physical processes and the ecology of a winter dinoflagellate bloom of Katodinium rotundatum. Mar Ecol Prog Ser 26:135−144.

Czypionka, T., et al. (2011). Importance of mixotrophic nanoplanctonin Aysén Fjord (Southern Chile) during austral winter. Cont Shelf Res 31: 216−224.

Edwards, K. F. (2019). Mixotrophy in nanoflagellates across environmental gradients in the ocean. Proc. Natl. Acad. Sci. 116: 6211–6220. doi:10.1073/pnas.1814860116.

U.S. EPA. (1993). Method 350.1: Nitrogen, Ammonia (Colorimetric, Automated Phenate). Revision 2.0. Cincinnati, OH.

U.S. EPA. (1993). Method 353.2: Nitrogen, Nitrate-Nitrite (Colorimetric, Automated Cadmium Reduction). Revision 2.0. Cincinnati, OH.

U.S. EPA. (1993). Method 365.1: Phosphorus, All Forms (Colorimetric, Automated Ascorbic Acid). Revision 2.0. Cincinnati, OH.

U.S. EPA. (1997). Method 366.0: Methods for determination of chemical substances in marine and estuarine matrices. Revision 1.0. Cincinnati, OH.

Faure, E., et al. (2019). Mixotrophic protists display contrasted biogeographies in the global ocean. ISME J. 13: 1072–1083. doi:10.1038/s41396-018-0340-5.

Fay, S. A., Gast, R. J., Sanders, R. W. (2013). Linking bacterivory and phyletic diversity of protists with a marker gene survey and experimental feeding with BrdU-labeled bacteria. Aquat Microb Ecol. 71:141−153.

Flynn, K. J., et al. (2013). Misuse of the phytoplankton - zooplankton dichotomy: the need to assign organisms as mixotrophs within plankton functional types. Journal of Plankton Research. 35(1), 3-11.

Fox, J. and Weisberg, S. (2016). Companion to applied regression. R package version 2.1-3. https://cran.r-project. org/package=car.

Friedrichs, C. T. (2009). York River Physical oceanography and sediment transport. Journal of Coastal Research, SI (57), 17-22.

Gast, R. J., Fay, S., Sanders, R. W. (2018). Mixotrophic activity and diversity of Antarctic marine protists in austral summer. Front. Mar. Sci. doi:10.3389/fmars.2018.00013.

Glibert, P. M., and Mitra, A. (2022). From webs, loops, shunts, and pumps to microbial multitasking: Evolving concepts of marine microbial ecology, the mixoplankton paradigm, and implications for a future ocean. Limnol. Oceanogr. 67: 585–597. doi:10.1002/lno.12018.

González, J. M. (1999). Bacterivory rate estimates and fraction of active bacterivores in natural protist assemblages from aquatic systems. *Appl Environ Microbiol.* 65:1463–1469.

Haraguchi, L., et al. (2018). Phytoplankton community dynamic: a driver for ciliate trophic strategies. Front Mar Sci. 5, 272.

Larsson, M. E, et al. (2022). Mucospheres produced by a mixotrophic protist impact ocean carbon cycling. Nature Communications. 13, 1301.

Leles, S.G., et al. (2019). Sampling bias misrepresents the biogeographical significance of constitutive mixotrophs across global oceans. Glob Ecol Biogeogr. 28, 418−428.

Li, Q. et al. (2021) Plasticity in the grazing ecophysiology of Florenciella (Dichtyochophyceae), a mixotrophic nanoflagellate that consumes Prochlorococcus and other bacteria. Limnol Oceanogr. 66:47−60.

Millette, N. C., et al. (2017). Mixotrophy in *Heterocapsa rotundata* : A mechanism for dominating the winter phytoplankton. Limnol. Oceanogr. 62: 836–845. doi:10.1002/lno.10470.

Millette, N. C., et al. (2018). Hidden in plain sight: The importance of cryptic interactions in marine plankton. Limnol. Oceanogr. Lett. 3: 341–356. doi:10.1002/lol2.10084.

Millette, N. C., et al. (2021). Temporal and spatial variability of phytoplankton and mixotrophs in a temperate estuary. Mar Ecol Prog Ser. 677, 17-31.

Mitra, A., et al. (2014). The role of mixotrophic protists in the biological carbon pump. *Biogeosciences* 11, 1–11.

Mitra, A., et al. (2023), The Mixoplankton Database – diversity of photo-phago-trophic plankton in form, function and distribution across the global ocean. J. Eukaryot. Microbiol. Accepted Author Manuscript e12972. https://doi.org/10.1111/jeu.12972.

Piredda, R., et al. (2017). Diversity and temporal patterns of planktonic protist assemblages at a Mediterranean Long Term Ecological Research site, *FEMS Microbiology Ecology*. 93:1. https://doi.org/10.1093/femsec/fiw200.

Reay, W. (2009). Water quality within the York River estuary. Journal of Coastal Research. 57,17-22. DOI:10.2112/1551-5036-57.sp1.23.

Sanders, R. W., and Gast, R. J. (2012). Bacterivory by phototrophic picoplankton and nanoplankton in Arctic waters. *FEMS Microbiol. Ecol.* 80, 242–253. doi: 10.1111/j.1574-6941.2011.01253.x.

Sanders, R., et al. (2000). Heterotrophic and mixotrophic nanoplankton predation on picoplankton in the Sargasso Sea and on Georges Bank. *Mar Ecol Prog Ser.* 192:103–118.

Sato, M., Shiozaki, T., Hashihama, F. (2017). Distribution of mixotrophic nanoflagellates along the latitudinal transect of the central North Pacific. *J Oceanogr.* 73:159–168.

Schneider, L.K., et al. (2020). Exploring the trophic spectrum: placing mixoplankton into marine protist communities of the southern North Sea. Front Mar Sci. 7.

Sherr, E. B., and Sherr B. F. (1993). Preservation and storage of samples for enumeration of heterotrophic protists. In: Kemp, P.F., Sherr, B.F., Sherr, E.B., Cole, J.J. (eds) Handbook of methods in aquatic microbial ecology. Lewis Publishers, Boca Raton, FL, 207−212.

Stoecker, D. K. (1998). Conceptual models of mixotrophy in planktonic protists and some ecological and evolutionary implications. Eur. J. Protistol. 34: 281–290. doi:10.1016/S0932-4739(98)80055-2.

Stoecker, D. K., et al. (2017). Mixotrophy in the Marine Plankton. Annu. Rev. Mar. Sci. 9: 311–335. doi:10.1146/annurev-marine-010816-060617.

Ward, B. A., and Follows, M. J. (2016). Marine mixotrophy increases trophic transfer efficiency, mean organism size, and vertical carbon flux. Proc Natl Acad Sci USA. 113, 2958−2963.

Wilken, S., et al.(2019). The need to account for cell biology in characterizing predatory mixotrophs in aquatic environments. Philos. Trans. R. Soc. B Biol. Sci. 374: 20190090. doi:10.1098/rstb.2019.0090.

Zuur, A. F., Ieno, E. N., Elphick, C. S. (2010). A protocol for data exploration to avoid common statistical problems. Methods Ecol Evol 1:3−14.

VITA

Born in Porto Alegre, Rio Grande do Sul, Brazil. Earned a B.S. in Biology from Saint Augustine's University in 2020. Entered a M.S. in Marine Science at the Virginia Institute of Marine Science / William & Mary in 2020. Currently a Sea Grant Knauss Fellow placed with NOAA NOS Formulation and Planning Division.